JGS
Journal of the Geological Society

Review article

Published online December 22, 2016 https://doi.org/10.1144/jgs2016-060 | Vol. 174 | 2017 | pp. 377–392

On the significance of short-duration regional metamorphism

Daniel Ricardo Viete[1]* & Gordon Stuart Lister[2]

[1] Department of Earth & Planetary Sciences, Johns Hopkins University, Baltimore, MD 21218, USA
[2] Research School of Earth Sciences, Australian National University, Canberra, ACT 0200, Australia
* Correspondence: viete@jhu.edu

Abstract: Short-duration regional metamorphism is a recently observed and poorly understood phenomenon in metamorphic geology. In this review, it is defined as metamorphism on time scales that limit length scales (of the associated thermal anomaly) to significantly less than the thickness of the orogenic crust (<10 myr) or subducted oceanic lithosphere (<5 myr). Without appealing to exceptional heat sources, thermal models have been unable to account for peak metamorphic temperature during collisional orogenesis and subduction. This observation, combined with restricted time scales for regional metamorphism, suggests that metamorphic facies series can record atypical and transient thermal conditions (related to punctuated and localized heat advection and/or production), rather than normal, ambient conditions for the tectonic setting to which they are allied. High-precision geochronology can resolve short-duration metamorphic estimates of 1 – 10 myr. However, diffusion geospeedometry typically yields extremely short metamorphic durations (<1 myr); tools in metamorphic geology may have matured to the point that the discipline is beginning to recognize episodicity and criticality in deep processes. New, very high-precision petrochronology techniques offer great potential to probe the veracity of extremely short metamorphic durations being obtained from diffusion geospeedometry. Benchmarking of these new very high-precision petrochronology techniques must become a priority for metamorphic geology.

Received 26 May 2016; **revised** 2 October 2016; **accepted** 27 October 2016

Early interpretations of the geological record leant heavily on catastrophism. As geology matured as a science, uniformitarianism came to supersede catastrophism. Uniformitarianism offers a more sophisticated, logical framework for interpretation of the rock record within the context of current and observable processes. However, the grand success of the uniformitarian philosophy has also resulted in a propensity toward interpretation of deep (and thus unobservable) geological phenomena in terms of slowly evolving or steady-state processes. A notable example of this preference for gradualism in deep processes has been ideas for the origins of regional metamorphism and metamorphic facies series, and implications for the nature of tectonism.

Barrow (1893, 1912) was the first to map regional metamorphism on the basis of diagnostic mineral assemblages. His Barrovian metamorphic sequence, exposed in NE Scotland, comprises a series of 'isograds' marking the first appearance of chlorite, biotite, garnet, staurolite, kyanite and sillimanite in pelitic lithologies, in the direction of increasing metamorphic grade. Regional metamorphism recorded by Barrovian-type isograds defines intermediate pressure/temperature (P/T) conditions (575 – 1250°C GPa^{-1}) that have occurred in association with continental collisional since the Archaean (Jamieson *et al.* 1998).

Barrow (1893) originally proposed that his Barrovian metamorphism resulted from magmatic advection of heat from depth. Following development of the theory of plate tectonics, numerous models were proposed for the origins of specific (e.g. Alpine, Barrovian, Himalayan, Zagros) examples of regional metamorphism in convergent settings (e.g. Oxburgh & Turcotte 1974; Bickle *et al.* 1975; Bird *et al.* 1975; Graham & England 1976; Richardson & Powell 1976; England & Richardson 1977; Toksöz & Bird 1977; England 1978). From these models, 'thermal relaxation' (England & Thompson 1984) emerged as an elegant and universal paradigm to explain the association between Barrovian-type metamorphism and collisional orogenesis. The thermal relaxation model for orogenic metamorphism posits that intermediate P/T conditions recorded by Barrovian-type regional metamorphism result from a return to crustal-scale thermal equilibrium following collision-related crustal thickening (with mantle heat flux at the base of the lithosphere, and modest rates of erosional exhumation and internal radiogenic heating).

In essence, the thermal relaxation model takes orogenic metamorphism to reflect relatively steady-state tectonothermal processes; regional metamorphism results, simply, from the long-term interplay of burial, erosion and internal (distributed) radiogenic heating. However, more recent work has demonstrated that Barrovian-type regional metamorphism requires exceptional crustal heating scenarios, involving localized regions of elevated radiogenic (e.g. Jamieson *et al.* 1998; Engi *et al.* 2001) or mechanical (e.g. England *et al.* 1992; Treloar 1997; Stüwe 1998; Burg & Gerya 2005) heat production, or fluid (e.g. Camacho *et al.* 2005; Dragovic *et al.* 2012, 2015), magmatic (e.g. Baxter *et al.* 2002; Brouwer *et al.* 2004; Reverdatto & Polyansky 2004; Viete *et al.* 2013) or tectonic (e.g. Smye *et al.* 2011; Ashley *et al.* 2015) heat advection, to account for peak metamorphic T. Globally, exceptional heating scenarios are also necessary to explain P–T conditions of subduction-zone metamorphism at forearc depths corresponding to $P < 2 – 2.5$ GPa (Penniston-Dorland *et al.* 2015).

Peak T attained in the roots of collisional orogens suggests that thermal relaxation is not a primary driver of Barrovian-type regional metamorphism. Time scales of regional metamorphism also support this position. Durations required for thermal relaxation in collisional orogens (involving heat conduction on the scale of overthickened crust) are of the order of 50 myr (e.g. Thompson & England 1984). As tools to interrogate durations of tectonism and associated regional metamorphism have improved, it has been repeatedly shown that time scales of thermal events recorded by regional metamorphism are too short to allow the crustal-scale heat conduction required by thermal relaxation (e.g. Oliver *et al.* 2000; Baxter *et al.* 2002; Dachs & Proyer 2002; Faryard & Chakraborty 2005; Ague & Baxter 2007; Smye *et al.* 2011; Viete *et al.* 2011*a*,*b*,

2013; Spear *et al.* 2012; Spear 2014). Moreover, examples of temporal non-uniformity in rates of metamorphism have been related to extremely short-duration thermal instabilities (tectono-metamorphic episodicity) within collisional orogens and subduction zones (e.g. Wijbrans & McDougall 1986, 1988; Keay *et al.* 2001; Kohn 2004; Camacho *et al.* 2005; Ague & Baxter 2007; Pollington & Baxter 2010; Viete *et al.* 2011*b*, 2015; Dragovic *et al.* 2012, 2015).

The emerging picture of short-duration and episodic metamorphism may have fundamental implications for exactly what metamorphism records (i.e. the 'everyday' versus the exceptional) and for what is 'typical' in terms of tectonic evolution. In this paper, the nature of regional metamorphism will be discussed and the concept of metamorphic facies series reviewed. First, however, to establish the geological significance of short-duration regional metamorphism, the following three questions must be addressed. (1) What qualifies as short-duration regional metamorphism? (2) Why is it geologically important? (3) Where and when has it occurred?

What qualifies as short-duration regional metamorphism?

Short-duration orogenic regional metamorphism, for the purpose of this review, is considered to involve a thermal excursion of duration 10^7 yr (10 myr) or less. (Metamorphism here is considered to involve thermal drivers and thus a *T* excursion. This need not always be the case; metamorphism may also be driven by *P* fluctuations (e.g. García-Casco *et al.* 2002; Forster & Lister 2005; Beltrando *et al.* 2007; Kabir & Takasu 2010; Rubatto *et al.* 2011; Lister & Forster 2016) and/or fluid fluxing (e.g. Bjørnerud *et al.* 2002; John *et al.* 2004; Bjørnerud & Austrheim 2006). Alternative metamorphic drivers and implications for large-scale, extremely short-duration metamorphism are briefly discussed later in this review.) Short-duration regional metamorphism in subduction zones is defined by a maximum thermal duration of 5 myr. The choice of 10 and 5 myr as upper limits for short-duration orogenic and subduction-zone metamorphism, respectively, is not arbitrary and the reasons relate to the geological importance of short-duration metamorphism.

Why is short-duration regional metamorphism geologically important?

Orogenic regional metamorphism involving durations less than 10 myr records a sub-crustal-scale thermal anomaly. Similarly, subduction-zone regional metamorphism with duration less than 5 myr records a sub-lithospheric-scale thermal anomaly. Thus, fundamentally, the associated thermal anomaly is transient and not reflective of the long-term tectonothermal environment.

There is currently little consensus on how the duration of a regional metamorphic event should be described. It is commonplace in diffusion geospeedometry to define a thermal event by a square-wave or triangular temperature–time (*T*–*t*) path. Although these approaches are relatively arbitrary, they are computationally simple and are valid for order-of-magnitude duration estimates. An alternative approach, used by Viete *et al.* (2011*a*), is to model conductive growth–decay of a thermal anomaly. The major advantage of this approach is that a *T*–*t* path (of fixed form) can be defined by a characteristic length scale of heat conduction, which can then be compared with field-determined dimensions of the regional metamorphic sequence (see Viete *et al.* 2011*a*).

Carslaw & Jaeger (1959) provided analytical solutions for the conduction of heat in solids, for various initial and boundary conditions. For most conductive heating scenarios, however, solutions are computationally awkward and require numerical modelling approaches. An alternative approach to modelling *T*–*t* evolution involves approximation of an infinite series solution to a conductive heating scenario of interest (e.g. Viete *et al.* 2011*a*). This approach can yield a simple equation that can be used to calculate a *T*–*t* curve for a given thermal diffusivity value and system size. Figure 1a describes temperature evolution at distance $x = L$, within an infinite half-space (i.e. 1D heating) composed of a material with thermal diffusivity *a*, following a heat pulse applied to the boundary at $x = t = 0$. A formula to describe the *T*–*t* curve of Figure 1a has been given by Viete *et al.* (2011*a*).

Because the conductive heating–cooling curve (Fig. 1a) displays exponential decay, time scales must be defined by some 'near-peak' duration above a *T* between ambient (T_{amb}) and maximum (T_{max}). As demonstrated in Figure 1b, the definition used for the 'near-peak' thermal duration (*t*) influences the associated conduction length scale (*L*). Figure 1c and d gives the relationship between *t* and *L* for the conductive heating–cooling curve of Figure 1a, a thermal diffusivity of $a = 10^{-6}$ m^2 s^{-1} and 'near-peak' thermal durations defined by time spent with *T* within the uppermost 30, 50, 70 and 90% of the total temperature excursion (Fig. 1b). For these conditions, a heating–cooling curve with defined duration $t = 10$ myr is produced by $L = 15 – 30$ km (see Fig. 1d).

The continental crust in active orogenic settings is typically >60 km in thickness (e.g. Pasyanos *et al.* 2014), meaning that a metamorphic event with 'near-peak' duration <10 myr will record a sub-crustal-scale thermal anomaly. Subducting oceanic lithosphere is typically >40 km in thickness (e.g. Turcotte & Schubert 2002; Pasyanos *et al.* 2014), meaning that lithospheric-scale thermal equilibrium in subduction settings must involve length scales >20 km and thus metamorphic time scales >5 myr (see Fig. 1d).

Consideration of *T*-dependent thermal diffusivity (e.g. Whittington *et al.* 2009), or internal radiogenic or mechanical heating, will lead to longer thermal time scales for a given conduction length scale. Similarly, protracted heating at $x = 0$, as may be expected for incremental (non-instantaneous) heat advection by thrusting, or episodic magmatism or fluid activity, will produce longer time scales for a given conduction length scale. On the other hand, advective cooling (e.g. erosional exhumation) may shorten thermal time scales for a given conduction length scale. Notwithstanding assumptions inherent in the approach outlined above and in Figure 1, definition of short-duration regional metamorphism as <10 myr for orogenic settings and <5 myr for subduction settings limits length scales of the associated thermal anomaly to significantly less than the thickness of the continental crust (in orogenic settings) or oceanic lithosphere (in subduction settings). Therefore, short-duration regional metamorphism is associated with crustal and/or lithospheric thermal disequilibrium marked by a localized thermal anomaly, meaning that it has fundamentally different geological significance to longer-duration metamorphism; additional heat sources (e.g. punctuated and localized heat advection and/or production) are required, and metamorphism is transient and anomalous rather than representing normal, ambient conditions for the tectonic setting to which it is allied.

Where and when has short-duration regional metamorphism occurred?

As a reference to the interested reader, and to support the arguments made in this review, two tables are provided. Table 1 gives a list of examples of regional metamorphism shown by high-precision geochronology to have developed over <10 myr for orogenic metamorphism and <5 myr for subduction-zone metamorphism. Estimates of age and *P*–*T* conditions for the metamorphism are also provided. Table 2 is equivalent to Table 1, but considers only duration estimates made on the basis of diffusion geospeedometry. Figure 2 shows the location and age of examples of short-duration metamorphism from Tables 1 and 2. Figure 3a and b illustrates metamorphic durations and *P*–*T* estimates for the studies from

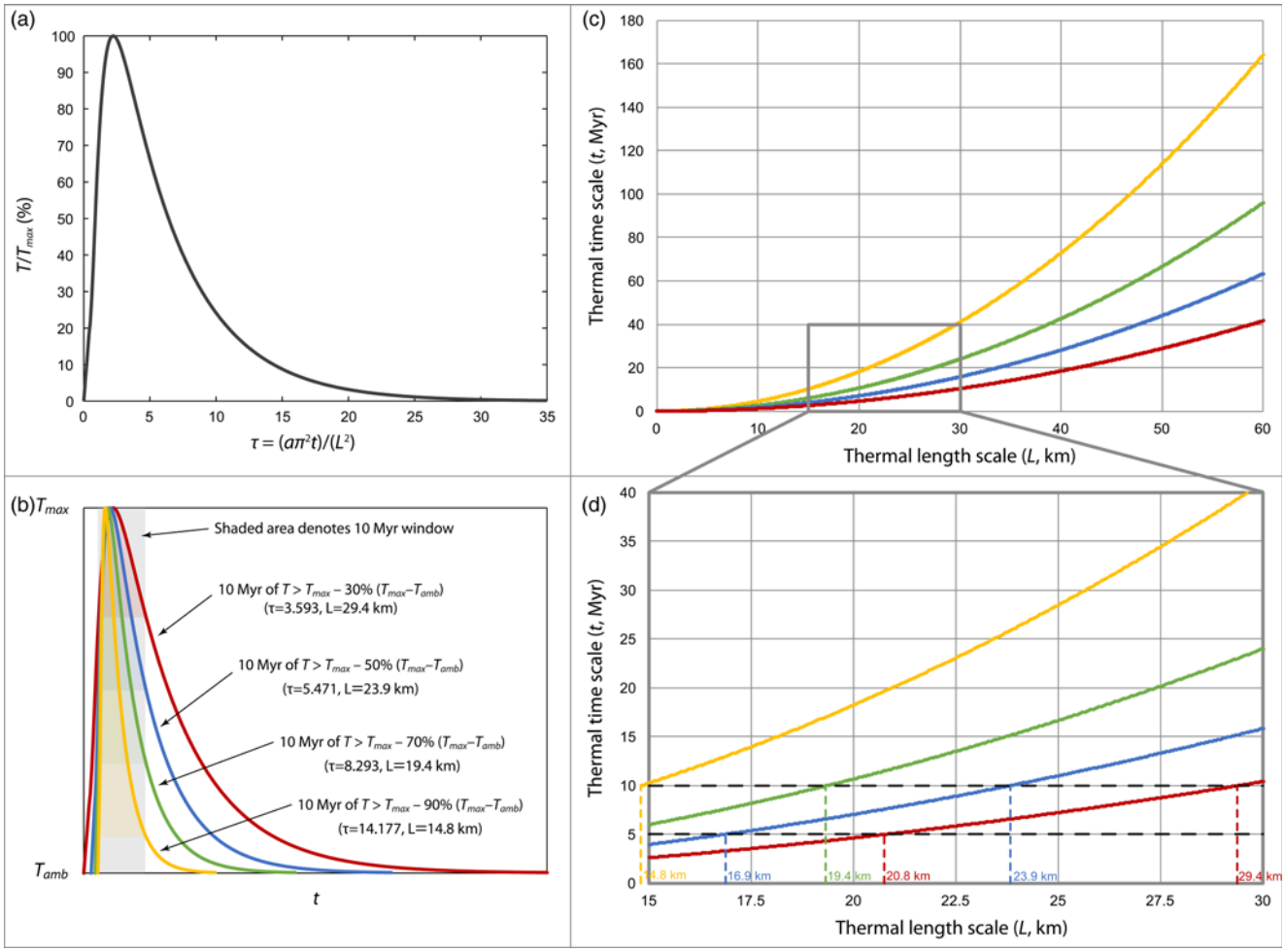

Fig. 1. (**a**) T evolution at $x = L$ for an infinite half-space with thermal diffusivity a, heated instantaneously at $x = t = 0$. Curve shows normalized temperature excursion (T/T_{max}) v. characteristic time (τ), and can be converted to T v. t by substituting values for T_{amb}, T_{max}, a and L. (**b**) Conductive T–t curves with the form of (**a**) for a 10 myr 'near-peak' thermal duration defined by time spent with T within the uppermost 30% (red), 50% (blue), 70% (green) and 90% (yellow) of the total temperature excursion (T_{max}–T_{amb}). (**c**) Thermal time scale, t, for varying conduction length scale, L. (**d**) Magnification of region of (**c**) of interest for short-duration orogenic metamorphism. Colours of curves in (**c**) and (**d**) correspond to those for the various definitions of duration of metamorphism in (**b**).

Tables 1 and 2, respectively. It should be noted that Tables 1 and 2, and Figures 2 and 3, although providing a relatively complete account of all published examples of short-duration regional metamorphism, are not exhaustive.

Although there are several examples of short-duration ultrahigh-temperature (UHT) metamorphism associated with large-scale magmatism (e.g. Platt *et al.* 1998; Schmitz & Bowring 2003; Kemp *et al.* 2007; Pownall *et al.* 2014), these are not included in Tables 1 and 2, and Figures 2 and 3. UHT metamorphism occurs at $T > 900$°C (Harley 1998) and, in the absence of obvious advective heat sources, requires highly radioactive source rocks, slow erosion rates and tens of million years to overcome the latent heat of partial melting (e.g. Clark *et al.* 2011, 2015; Horton *et al.* 2016). Moreover, even the most robust geochronometers (e.g. zircon, monazite, rutile) experience dissolution–precipitation and post-crystalline resetting at UHT conditions (e.g. Kelsey 2008; Kelsey & Hand 2015; Harley 2016), adding great complexity to efforts to constrain time scales for UHT metamorphism. Durations and drivers for UHT metamorphism are beyond the scope of this review, and the interested reader is referred to the detailed reviews of Kelsey & Hand (2015) and Harley (2016).

Tables 1 and 2 list dozens of examples of regional metamorphism with duration so brief as to record transient, anomalous thermal conditions. These include many classic examples of regional metamorphism (e.g. the Alps, Greek Cyclades, Himalaya, New England, Scotland). The metamorphic facies series concept considers regional metamorphism to record relatively long-lived tectonothermal environments. Thus, the prevalence of short-duration regional metamorphism has significant implications for the metamorphic facies series concept, which links metamorphic geology and plate tectonics.

The metamorphic facies series concept

Metamorphic rocks provide the most reliable record of thermal conditions in the crust. Thermodynamic datasets amassed from extensive experimental work (e.g. Berman 1988; Holland & Powell 1990, 1998, 2011) are routinely used to calculate metamorphic P and T from the metastable minerals and mineral assemblages that form metamorphic rocks. Despite firm understanding of P–T conditions for metamorphism, important questions remain regarding why metamorphism occurs when it does and exactly what it records.

Current techniques for estimating metamorphic P–T conditions follow from the early concept of metamorphic facies (Eskola 1915, 1920). Barrow (1893, 1912) demonstrated that an increasing degree of metamorphism is reflected in a succession of mineral assemblages in pelites, defining his Barrovian metamorphic

Table 1. *Worldwide examples of regional metamorphism for which high-precision geochronology produced a metamorphic duration estimate of less than 5–10 myr*

Location	Metamorphic facies, facies series	Approximate *T* (°C), *P* (GPa)	Age range (Ma)	Duration (myr), Duration used in Figure 1 (myr)	Isotope system	Reference
Kaghan Valley, Pakistan Himalaya*	UHP, Franciscan	725, 2.9	46 – 44	2 – 4, 3	U–Pb rt	Treloar *et al.* (2003)
Kaghan Valley, Pakistan Himalaya*	UHP, Franciscan	745, 2.75	46.5 – 44.1	0.4 – 4.4, 2.4	U–Pb aln, U–Pb zrn	Parrish *et al.* (2006)
Sifnos, Cyclades, Aegean Sea, Greece	Eclogite, Franciscan	560, 2.2	46.5 – 46.5	<1.0, 1	Sm–Nd grt	Dragovic *et al.* (2012)
Sifnos, Cyclades, Aegean Sea, Greece	Eclogite, Franciscan	520, 2.1	47.2 – 45	1.5 – 3, 2.2	Sm–Nd grt	Dragovic *et al.* (2015)
Syros, Cyclades, Aegean Sea, Greece	Eclogite, Franciscan	500, 1.5	52.2 – 50	<4.5, 2.2	Lu–Hf grt	Lagos *et al.* (2007)
Syros, Cyclades, Aegean Sea, Greece	Eclogite, Franciscan	500, 2.2	53.1 – 51.2	2, 2	Ar–Ar wm	Lister & Forster (2016)
D'Entrecasteaux Metamorphic Core Complex, D'Entrecasteaux Islands, SE Papua New Guinea	Eclogite, Franciscan	900, 2.2	4.3 – 0	<4, 1	U–Pb zrn	Baldwin *et al.* (2004)
Sesia Zone, W Alps, Italy*	Eclogite, Franciscan	580, 2.2	78.5 – 75.6	1.2 – 4.6, 2.9	U–Pb aln, U–Pb zrn	Rubatto *et al.* (2011)
Sesia Zone, W Alps, Italy*	Eclogite, Franciscan	560, 2.0	69 – 65	<10, 4	U–Pb ttn, U–Pb zrn	Rubatto *et al.* (2011)
Yukon–Tanana Terrane, S Yukon, Canada	Eclogite, Sanbagawan	690, 1.5	264 – 256	<8, 4	Lu–Hf grt, Ar–Ar wm	Philippot *et al.* (2001)
Sesia Zone, W Alps, Italy*	Eclogite (overprint), Sanbagawan	550, 1.2	76 – 69.8	4.4 – 8, 6.2	U–Pb aln, U–Pb zrn	Rubatto *et al.* (2011)
Tauern Window, E Alps, Austria*	Eclogite (overprint), Sanbagawan	550, 1.1	32 – 28	4, 4	U–Pb aln	Smye *et al.* (2011)
Tauern Window, E Alps, Austria	Epidote amphibolite (overprint), Barrovian	550, 0.9	27.5 – 20	7 – 8, 7.5	Sm–Nd grt	Pollington & Baxter (2010)
Upper Schieferhülle, Tauern Window, E Alps, Austria	Epidote amphibolite (overprint), Barrovian	475, 0.4	35.4 – 30	3.7 – 7.1, 5.4	Rb-Sr grt	Christensen *et al.* (1994)
Dora Maira Massif, W Alps, Italy	Epidote amphibolite (overprint), Barrovian	570, 1.0	35.1 – 31.8	2 – 4.8, 3.4	U–Pb ttn	Rubatto & Hermann (2001)
Franja Costera Unit, Cordillera de la Costa, Puerto Cabello, north–central Venezuela	Epidote amphibolite (overprint), Barrovian	580, 1.0	33.5 – 32.5	0.5 – 2, 1	U–Pb ttn, U–Pb zrn	Viete *et al.* (2015)
Steinental Area, Lepontine Alps, Switzerland	Epidote amphibolite, Barrovian	520, 0.64	32 – 24.9	4 – 10, 7	Rb–Sr grt	Vance & O'Nions (1992)
South Armenian Block, Armenia	Epidote amphibolite, Barrovian	575, 0.8	160 – 155	5, 5	U–Pb zrn, Ar–Ar wm	Hässig *et al.* (2015)
Wepawaug Schist, Orange–Milford Belt, S Connecticut, USA	Epidote amphibolite, Barrovian	610, 0.9	389 – 380	6 – 12, 9	Sm–Nd grt	Lancaster *et al.* (2008)
Pinney Hollow Formation, Townshend Dam, SE Vermont, USA	Epidote amphibolite, Barrovian	600, 0.95	380.3 – 376.5	1.6 – 6, 3.8	Sm–Nd grt	Gatewood *et al.* (2015)
Ottauque Formation, SE Vermont, USA	Epidote amphibolite, Barrovian	500, 0.5	380 – 369.5	6.3 – 14.7, 10	Rb–Sr grt	Christensen *et al.* (1989)
Lesser Himalayan Formation, Central Himalaya, Nepal	Epidote amphibolite, Barrovian	535, 0.72	3.3 – 0	<3.3, 2	U–Pb mnz	Catlos *et al.* (2001)
Lesser Himalayan Formation, Central Himalaya, Nepal	Epidote amphibolite, Barrovian	550, 0.7	6 – 0	<6, 3	Th–Pb mnz	Harrison *et al.* (1997)
Fleur de Lys Supergroup, Newfoundland, Canada	Epidote amphibolite, Barrovian	530, 0.61	448.4 – 448.6	0.33 – 4.7, 2.5	Rb–Sr grt, Sm–Nd grt	Vance & O'Nions (1990)
Skaiti Supergroup, Sulitjelma, N Norway	Greenschist, Barrovian	460, 0.52	434.1 – 424.6	7.1 – 11.9, 9.5	Sm–Nd grt	Burton & O'Nions (1991)
Blyb Metamorphic Complex, Great Caucasus, Russia	Amphibolite (overprint), Barrovian	660, 0.8	316 – 303	<8, 4	Lu–Hf grt, Ar–Ar wm	Philippot *et al.* (2001)
Lesser Himalayan Formation, Sikkim Himalaya, India	Amphibolite, Barrovian	660, 0.9	20.8 – 15.6	4.8 – 5.6, 5.2	U–Pb mnz	Mottram *et al.* (2014)
Lesser Himalayan Formation, Sikkim Himalaya, India	Amphibolite, Barrovian	660, 0.9	21 – 16	5, 5	U–Pb zrn, Ar–Ar wm	Mottram *et al.* (2015)

(continued)

Table 1. *(Continued)*

Location	Metamorphic facies, facies series	Approximate T (°C), P (GPa)	Age range (Ma)	Duration (myr), Duration used in Figure 1 (myr)	Isotope system	Reference
Barrovian Series, E Scotland	Amphibolite, Barrovian	690, 0.6	473 – 465	8, 8	U–Pb zrn	Viete *et al.* (2013)
Barrovian Series, E Scotland	Amphibolite, Barrovian	660, 0.6	473 – 465	3 – 13, 8	Sm–Nd grt	Baxter *et al.* (2002)
Barrovian Series, E Scotland	Amphibolite, Barrovian	650, 0.75	472 – 465	3 – 11, 7	Sm–Nd grt	Oliver *et al.* (2000)
Barrovian Series, E Scotland	Amphibolite, Barrovian	750, 1.0	472 – 468	<13, 8	U–Pb zrn	Vorhies *et al.* (2013)
E Chugach Metamorphic Complex, S Alaska, USA*	Amphibolite, Barrovian	660, 0.9	52 – 50	2, 2	U–Pb zrn	Gasser *et al.* (2012)
W Chugach Metamorphic Complex, S Alaska, USA*	Amphibolite, Barrovian	670, 0.8	55 – 52	3, 3	U–Pb zrn	Gasser *et al.* (2012)
Salinian Terrane, California	Amphibolite, Barrovian	750, 0.8	78.2 – 77.9	<6, 3	Sm–Nd grt	Ducea *et al.* (2003)
Shuswup Metamorphic Core Complex, Thor–Odin Dome, British Columbia, Canada*	Amphibolite, Barrovian	700, 0.65	59.8 – 55.9	<8, 4	U–Pb zrn	Vanderhaeghe *et al.* (1999)
Wenatchee Block, Cascades Crystalline Core, Washington, USA	Amphibolite, Barrovian	650, 0.7	92 – 86	<6, 6	Sm–Nd grt	Stowell *et al.* (2011)
Niğde Massif, Central Anatolian Crystalline Complex, Central Turkey	Amphibolite, Barrovian	725, 0.6	92 – 85	3.5 – 9, 6	U–Pb mnz, U–Pb zrn	Whitney *et al.* (2003)
Higher Himalayan Crystalline Series, Sikkim, India	Granulite, Barrovian	800, 0.85	31 – 27	4, 4	U–Pb mnz, U–Pb zrn	Rubatto *et al.* (2013)
Higher Himalayan Crystalline Series, Sikkim, India	Granulite, Barrovian	800, 0.85	26 – 23	3, 3	U–Pb mnz, U–Pb zrn	Rubatto *et al.* (2013)
Valhalla Complex, British Columbia, Canada	Granulite, Barrovian	820, 0.8	67.3 – 60.9	2 – 10.8, 6.4	Sm–Nd grt	Ducea *et al.* (2003)
Naxos, Cyclades, Aegean Sea, Greece	Granulite, Buchan	675, 0.3	20.7 – 16.8	3.9, 3.9	U–Pb zrn	Keay *et al.* (2001)

Information is provided on location, metamorphic facies and facies series, approximate metamorphic P–T conditions, age, geochronometer used and reference. Mineral abbreviations after Kretz (1983); wm, white mica; UHP, ultrahigh-pressure.
*Regional studies that report short-duration regional metamorphism on the basis of comparison of ages obtained from multiple rocks collected from structurally distinct lithotectonic units and/or units separated by significant along-strike distances.

sequence. Eskola (1915, 1920) extended Barrow's findings, proposing that fields in P–T space (metamorphic facies) can be delineated by commonly observed metamorphic mineral associations. Figure 3 illustrates the P–T range and distribution of the most commonly accepted metamorphic facies (e.g. Miyashiro 1973; Turner 1981; Spear 1993).

With the advent of the theory of plate tectonics, the metamorphic facies concept was extended to that of metamorphic facies series (Miyashiro 1961, 1973). Miyashiro (1961, 1973) recognized that specific tectonic settings are associated with metamorphic facies defining distinct P/T arrays. With respect to an assumed stable crustal geotherm (e.g. Rudnick *et al.* 1998), facies series associated with regional metamorphism can be divided into low P/T, intermediate P/T, intermediate–high P/T and high P/T (Miyashiro 1961, 1973). Rates of tectonic processes outstrip those of the conduction of heat in rock, meaning that specific quasi-steady-state thermal environments would logically emerge from the processes of large-scale advection (e.g. crustal thickening, thinning, subduction) that characterize plate tectonics. Quantitative modelling of tectonic advection and crustal heat flow supports this idea (e.g. McKenzie 1967, 1969; England & Thompson 1984).

In this review paper, low, intermediate, intermediate–high and high P/T are referred to with respect to the classic examples of metamorphism of low P/high T (Buchan of Read 1923, 1952), medium P/medium T (Barrovian of Barrow 1893, 1912), high P/medium T (Sanbagawan of Miyashiro 1961, 1973) and high P/low T (Franciscan of Bailey 1962; Ernst 1963; Bailey *et al.* 1964). In Figure 3, Buchan-type (low P/T) metamorphism has T–P ratios >1250°C GPa^{-1}, meaning that andalusite (rather than kyanite) occurs as the low-T aluminosilicate phase and the metamorphic facies progression is typified by zeolite–greenschist–amphibolite–granulite. Franciscan-type (high P/T) metamorphism is considered to involve T–P ratios <425°C GPa^{-1} and zeolite–prehnite pumpellyite–blueschist–eclogite facies assemblages (Fig. 3). Barrovian-type (intermediate P/T) metamorphism has T–P ratios of 575 – 1250°C GPa^{-1}, restricting aluminosilicate phases to kyanite and sillimanite, and metamorphic assemblages to zeolite–(prehnite pumpellyite–)greenschist–epidote amphibolite–amphibolite–granulite facies (Fig. 3). Finally, this review paper considers Sanbagawan-type (intermediate-high P/T) metamorphism to comprise a narrow band of T–P ratios (425 – 575°C GPa^{-1}) that produces greenschist- or blueschist-facies assemblages at T = 250 – 450°C and eclogite-facies assemblages at T > 675°C (Fig. 3). The type Sanbagawan metamorphic series preserves a progression with increasing T from blueschist to greenschist and/or epidote amphibolite facies then eclogite facies (see Miyashiro 1994, rfig. 8.3, p. 203). Unlike for the other metamorphic facies series, intermediate-high P/T metamorphism will not necessarily preserve the exact metamorphic facies progression observed for its type locality.

Eskola (1939) and various researchers since (e.g. Miyashiro 1973, 1994; Turner 1981; Yardley 1989) recognize an extremely low P/T contact metamorphic facies series comprising a facies progression of albite epidote hornfels–hornblende hornfels–pyroxene hornfels–sanadinite. Low P/T, Buchan-type metamorphism is related to magmatism and associated advection of heat into the upper crust (e.g. Wickham & Oxburgh 1985; Barton & Hanson 1989; De Yoreo *et al.* 1991; Sandiford & Powell 1991; Collins 2002; Viete *et al.* 2010). The contact metamorphic facies series may thus be viewed as a very localized and extreme member of the Buchan metamorphic facies series.

Table 2. *Worldwide examples of regional metamorphism for which diffusion geospeedometry produced a metamorphic duration estimate of <10 myr*

Location	Metamorphic facies	Approximate *T* (°C), *P* (GPa)	Age	Duration, Duration used in Figure 1 (kyr)	Diffusion system	Arrhenius parameters	Reference
Bergen Arcs, SW Norway	Eclogite, Franciscan	720, 2.0	Scandian, *c.* 425 Ma	17 – 32 kyr, 25	Ca, Fe, Mg in grt	Ganguly *et al.* (1998)	Raimbourg *et al.* (2007)
Bergen Arcs, SW Norway	Eclogite, Franciscan	525, 1.9	Scandian, *c.* 423 Ma	18 kyr, 18	Ar in hbl, phl	Giletti (1974), Harrison (1981)	Camacho *et al.* (2005)
Tauern Window, E Alps, Austria	Eclogite, Franciscan	570, 1.7	Alpine, *c.* 34 Ma	100 – 500 kyr, 300	Fe, Mn in grt	Loomis *et al.* (1985), Chakraborty & Ganguly (1992)	Dachs & Proyer (2002)
NW Connecticut, New England, NE USA	Eclogite, Sanbagawan	710, 1.45	Taconian, *c.* 455 Ma	Comparative (<10), 10*	Mn in grt	n.a.	Chu *et al.* (2016)
Yukon–Tanana Terrane, S Yukon, Canada	Eclogite, Sanbagawan	690, 1.5	Klondike, *c.* 259 Ma	200 kyr, 200	Ca in grt	Schwandt *et al.* (1996)	Perchuk *et al.* (1999)
Eastern Vermont, New England, NE USA	Greenschist, Barrovian	450, 0.75	Acadian, *c.* 364 Ma	<1 – 200 yr, 0.1	Fe in cal	Müller *et al.* (2012)	Ferry *et al.* (2015)
Region of Moine Thrust, N Scotland	Epidote amphibolite, Barrovian	590, 0.7	Scandian, *c.* 425 Ma	<100 – 200 kyr, 100	Ti in qtz	Cherniak *et al.* (2007)	Ashley *et al.* (2015)
Middle Austroalpine Unit, E Alps, Austria	Epidote amphibolite (overprint), Barrovian	600, 1.0	Eo-Alpine, *c.* 94 Ma	800 – 900 kyr, 850	Ca, Fe, Mg, Mn in grt	Chakraborty & Ganguly (1992)	Faryard & Chakraborty (2005)
Central Vermont, New England, NE USA	Epidote amphibolite, Barrovian	640, 1.0	Acadian, *c.* 353 Ma	0.12 – 1.8 myr, 1000	Mn in grt	Chakraborty & Ganguly (1992)	Spear (2014)
Central Vermont, New England, NE USA	Amphibolite, Barrovian	580, 0.51	Acadian, *c.* 353 Ma	0.2 – 2 myr, 1000	Ti in qtz	Cherniak *et al.* (2007)	Spear *et al.* (2012)
Moldanubian Zone, Bohemian Massif, Světlík area, Czech Republic	Amphibolite (overprint), Barrovian	710, 0.73	Variscan, *c.* 375 Ma	<200 kyr, 100	Fe in grt	Chakraborty & Ganguly (1992)	O'Brien & Vrana (1995)
Moldanubicum, Bohemian Massif, NW Ottenschlag, Lower Austria	Amphibolite (overprint), Barrovian	725, 0.8	Variscan, *c.* 375 Ma	100 – 700 kyr, 500	Ca, Fe, Mg in grt	Chakraborty & Ganguly (1992)	O'Brien (1997)
Blyb Metamorphic Complex, Great Caucasus, Russia	Amphibolite (overprint), Barrovian	660, 0.8	Variscan, *c.* 310 Ma	100 – 500 kyr, 300	Mg in grt	Chakraborty & Rubie (1996)	Perchuk & Philippot (2000)
Blyb Metamorphic Complex, Great Caucasus, Russia	Amphibolite (overprint), Barrovian	660, 0.8	Variscan, *c.* 310 Ma	0.5 – 2.5 myr, 1000	Mg in grt	Chakraborty & Rubie (1996)	Perchuk & Philippot (1997)
Barrovian Series, E Scotland	Amphibolite, Barrovian	640, 0.59	Grampian, *c.* 470 Ma	Comparative (10 – 100 kyr episodes), 50†	Mn, Ca in grt	n.a.	Viete *et al.* (2011*b*)
Barrovian Series, E Scotland	Amphibolite, Barrovian	660, 0.57	Grampian, *c.* 470 Ma	30 – 200 kyr, 100	Ca, Fe, Mg, Mn in grt	Carlson (2006)	Ague & Baxter (2007)
Barrovian Series, E Scotland	Amphibolite, Barrovian	600, 0.5	Grampian, *c.* 470 Ma	<2 myr, 750	Ca, Fe, Mg, Mn in grt	Chu & Ague (2015)	Chu & Ague (2015)
Barrovian Series, E Scotland	Amphibolite, Barrovian	660, 0.6	Grampian, *c.* 470 Ma	Comparative (10–20 times longer than Himalayan), n.a.‡	Mn in grt	n.a.	Ayres & Vance (1997)
Higher Himalayan Crystalline Series, Zanskar Himalaya, NW India	Amphibolite, Barrovian	690, 1.0	Himalayan, *c.* 33 Ma	Comparative (10–20 times shorter than Barrovian), n.a.‡	Mn in grt	n.a.	Ayres & Vance (1997)
Maine, New England, NE USA	Greenschist, Buchan	450, 0.35	Acadian, *c.* 364 Ma	<1 – 200 yr, 0.1	Fe in cal	Müller *et al.* (2012)	Ferry *et al.* (2015)
Barrovian Series, E Scotland	Greenschist, Buchan	475, 0.33	Grampian, *c.* 470 Ma	1 – 10 myr, 5000	Ar in wm	Harrison *et al.* (2009)	Viete *et al.* (2011*a*)
Barrovian Series, E Scotland	Amphibolite, Buchan	565, 0.4	Grampian, *c.* 470 Ma	200 – 500 kyr, 300	Sr in ap	Cherniak & Ryerson (1993)	Ague & Baxter (2007)

Information is provided on location, metamorphic facies and facies series, approximate metamorphic *P–T* conditions, age, diffusion system, Arrhenius parameters used and reference. Mineral abbreviations after Kretz (1983); wm, white mica; n.a., not applicable.

*Compared with diffusion length scale over 1 myr at 660°C.

†Metamorphic episodes of 10 – 100 kyr punctuate the 1 – 10 myr Barrovian regional metamorphism.

‡Relative length scales of diffusion suggest that Barrovian metamorphism in Scotland developed over a duration 10–20 times longer than Himalayan Barrovian-type metamorphism.

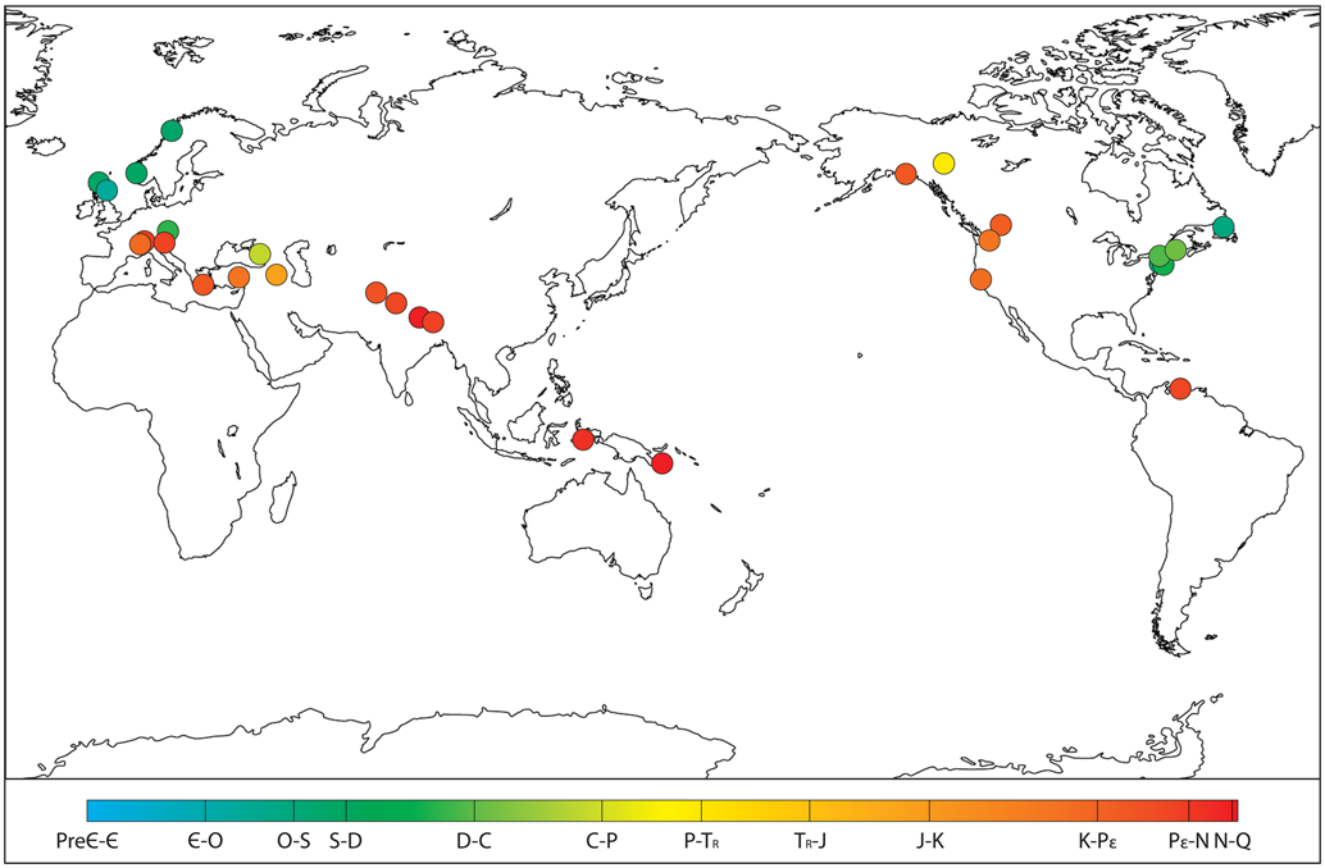

Fig. 2. Locations of some worldwide examples of short-duration metamorphism. Colour denotes age (from the beginning of the Palaeozoic). Only selected examples from Tables 1 and 2 are shown to avoid overcluttering.

Barrovian-, Sanbagawan- and Franciscan-type metamorphism is often taken to reflect relatively steady-state thermal processes within the tectonic environments with which they are associated. As discussed above with respect to the importance of short-duration regional metamorphism, brief heating (i.e. <5 – 10 myr) limits thermal length scales, meaning that associated metamorphic facies series do not represent a stable tectonothermal environment. Instead, metamorphic facies series produced by short-duration regional metamorphism represent some *P–T* conditions arising in response to punctuated and localized processes of heat advection and/or production. Jamieson *et al.* (1998, p. 23), with reference to global examples of orogenic regional metamorphism, asked: 'Barrovian regional metamorphism: where's the heat?' Penniston-Dorland *et al.* (2015, p. 243), with reference to global examples of subduction-zone metamorphism, exclaimed 'rocks are hotter than models'. Metamorphic rocks record excessive *T* for the steady-state tectonothermal scenarios with which they are associated, and short-duration regional metamorphism, fundamentally, records thermal transience.

The picture emerging from *P–T* conditions and durations of regional metamorphism suggests that metamorphic facies series do not necessarily record steady-state thermal processes for the tectonic environment to which they are allied. If what is recorded by regional metamorphism is typically 'exceptional' rather than 'normal', then this leads to questions concerning the significance of metamorphism and metamorphic rocks, and potential bias in the exhumed rock record. Are metamorphic rocks really representative of the long-term/quasi-steady-state thermal picture of the crust? Is exhumation/preservation of transient thermal conditions (metamorphism) preferred and, if so, why? Do metamorphic facies series have the geological significance they are thought to have?

Metamorphic facies series are used as a primary tool for understanding the thermal state of the crust and how the processes of plate tectonics move heat; the concept of metamorphic facies series links metamorphic geology and plate tectonics. Thus, answers to the questions above have potential to reframe the entire discipline of metamorphic geology and its role in the understanding of our planet.

Figure 2 shows that metamorphic duration estimates from diffusion geospeedometry are significantly shorter than those obtained from high-precision geochronology. Additionally, Tables 1 and 2 and Figure 3 contain no Precambrian examples of short-duration metamorphism. These observations highlight limitations in existing approaches to estimating metamorphic duration. Below, the phenomenon of extremely short-duration (i.e. <1 myr) metamorphism is introduced, and its implications for the nature of metamorphism and episodicity in deep processes are discussed. Within the context of extremely short-duration metamorphism, opportunities offered by new techniques for quantifying short-duration metamorphism are also reviewed.

Extremely short-duration metamorphism

Most examples of short-duration metamorphism in Figure 2 are very young (late Mesozoic–Tertiary), and there are no Archaean or Proterozoic examples. Secular changes in thermal state and/or crustal chemistry may have limited intermediate–high and high *P*/*T* metamorphism during the Precambrian (e.g. Stern 2005; Palin & White 2016). In addition, with reworking of the continental crust, one may expect higher preservation potential for younger low and intermediate *P*/*T* regional metamorphic sequences. However, perhaps the most convincing explanation for the lack of known examples of Precambrian short-duration metamorphism is that uncertainties in geochronology limit temporal resolution in old rocks. For example, 2% uncertainty precludes recognition of

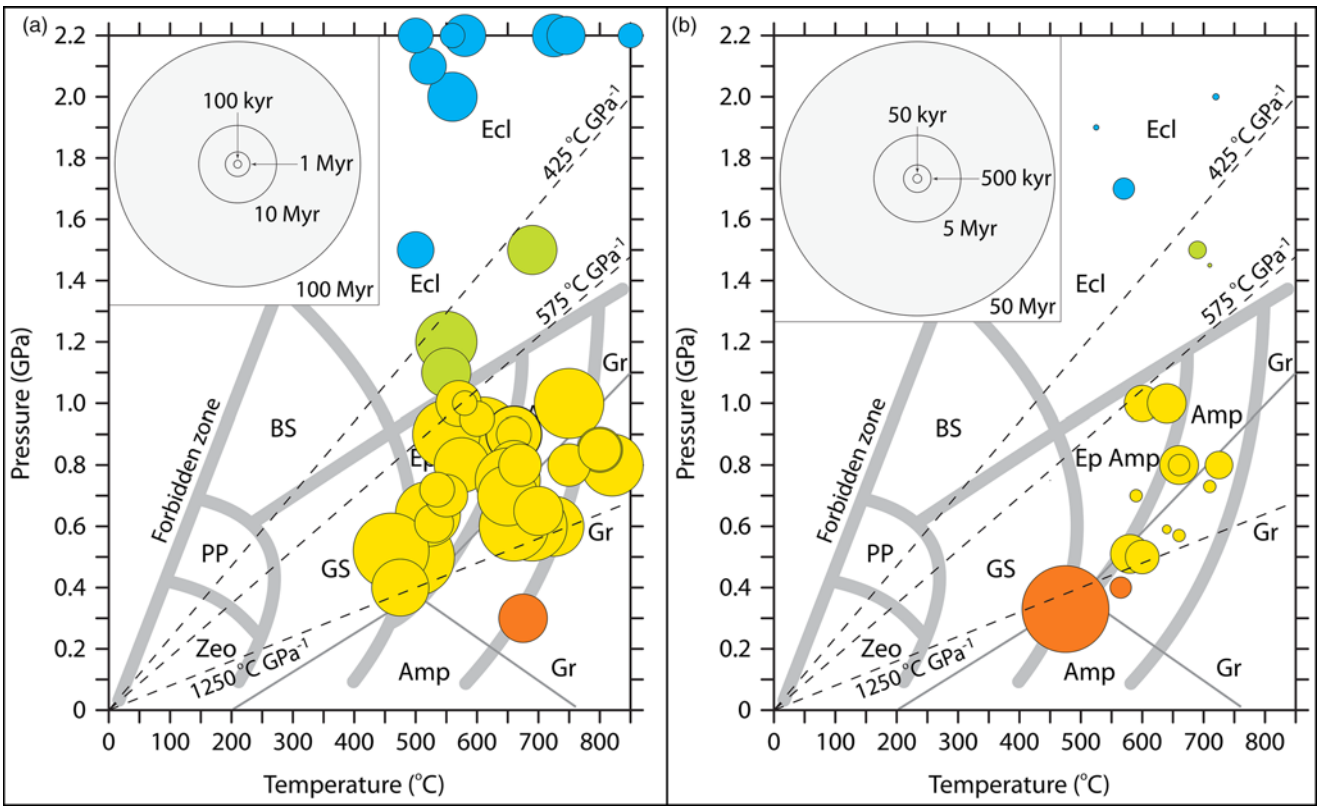

Fig. 3. *P–T* conditions for short-duration metamorphism from (**a**) Table 1, based on high-precision geochronology, and (**b**) Table 2, based on diffusion geospeedometry. The area of each circle gives metamorphic time scale, meaning that the diameter gives the conduction length scale ($L \propto \sqrt{t}$). Inset at top left of (**a**) and (**b**) provides a key for time scale comparison; it should be noted that, for the same circle size, duration is longer for (**a**) than for (**b**). Orange, yellow, green and blue symbols denote rocks belonging to the Buchan (low *P*/*T*), Barrovian (imtermediate *P*/*T*), Sanbagawan (intermediate–high *P*/*T*) and Franciscan (high *P*/*T*) metamorphic facies series, respectively. Metamorphic facies: Zeo, zeolite; PP, prehnite–pumpellyite; GS, greenschist; BS, blueschist; Ecl, eclogite; Ep Amp, epidote amphibolite, Amp, amphibolite; Gr, granulite; and aluminosilicate fields (fine continuous lines) after Spear (1993, fig. 2-2, p. 17). Papua New Guinea eclogite example of Baldwin *et al.* (2004) is plotted at 850°C rather than 900°C. Himalayan ultrahigh-pressure (UHP) examples of Treloar *et al.* (2003) and Parrish *et al.* (2006) are plotted at 2.2 GPa rather than 2.75 – 2.9 GPa.

short-duration metamorphism (<10 myr) in rocks older than *c.* 500 Ma. Although short-duration metamorphism may have been commonplace in the Precambrian, current tools may not allow its recognition.

The key to extending knowledge of short-duration metamorphism into the Precambrian may be diffusion geospeedometry. However, diffusion geospeedometry approaches also have their pitfalls. A comparison of Figure 3a and b is revealing; duration estimates from diffusion geospeedometry are significantly and systematically shorter than those obtained from high-precision geochronology. This observation conflates two potential influences: limitations in temporal resolution may cause approaches in geochronology to overestimate metamorphic time scales (particularly for Palaeozoic rocks), whereas uncertainties in the Arrhenius parameters that govern diffusion or invalid assumptions inherent in diffusion models (such as the form of the initial composition profile, redox conditions during metamorphism or premise of mechanical equilibrium) may cause approaches in diffusion geospeedometry to underestimate metamorphic time scales.

Metamorphism involving time scales <1 myr, obtained exclusively from diffusion geospeedometry (Fig. 3), is here referred to as extremely short-duration metamorphism. It is important to establish whether the short time scales of regional metamorphism obtained from high-precision geochronology (typically 1 – 10 myr; Fig. 3a) or extremely short time scales obtained from diffusion geospeedometry (typically 10 – 1000 kyr; Fig. 3b) are typical of short-duration regional metamorphism. This is because extremely short-duration metamorphism may have great implications not only for the significance of metamorphic facies series and the tectonic picture provided by metamorphic rocks, but also for metamorphic drivers. The key to exploring this issue will be more detailed experimental work to explore the full range of variables that influence diffusion rates, in addition to the development of new very high-precision, petrologically controlled techniques in geochronology that are capable of estimating metamorphic duration and verifying estimates obtained from diffusion geospeedometry.

Diffusion rates: experiments and models versus nature

For given chemical conditions, chemical diffusion is a temperature- and pressure-dependent process. The Arrhenius equation (equation (1)) describes diffusion rates in terms of *T*, *P*, frequency factor, D_0, activation energy, *Q*, and activation volume, ΔV^+:

$$D = D_0 \exp\left[\frac{-(Q + P\Delta V^+)}{RT}\right]. \quad (1)$$

D_0, *Q* and ΔV^+, collectively, are the Arrhenius parameters for diffusion. Diffusion geospeedometry involves forward modelling to reproduce observed length scales of chemical diffusion. Results obtained from forward modelling are dependent on various assumptions, relating to (1) initial and boundary conditions for diffusion, (2) the (*P*–)*T*–*t* path for metamorphism (rightly or wrongly, the influence of *P* is commonly ignored) and (3) Arrhenius parameters. Most commonly, Arrhenius parameters are determined experimentally, allowing chemistry, *T* and *P* to be prescribed. However, to ensure experiments are completed within a reasonable time frame (i.e. weeks to months), they must be performed at high *T* (and often low *P*). Down-temperature extrapolation of the results of

diffusion experiments can introduce significant (order of magnitude) errors (e.g. Chu & Ague 2015). Arrhenius parameters have also been estimated from forward modelling to reproduce stranded chemical diffusion profiles in natural rocks (e.g. Carlson 2006), but this approach is an inversion of diffusion geospeedometry, and is thus plagued by uncertainty relating to initial and boundary conditions for diffusion and the (*P*–)*T*–*t* history of the rocks.

Metamorphic duration estimates obtained from diffusion geospeedometry are shorter than those obtained from high-precision geochronology (Fig. 3). Thus, if down-temperature extrapolation of Arrhenius parameters is contributing to this mismatch, then the associated errors must arise from systematic experimental overestimation of natural diffusion rates (e.g. Baxter 2003; Villa 2006, 2016); either mechanisms for diffusion are fundamentally different from what we envision and reproduce in experiments, or experiments consistently misrepresent the chemical and physical conditions found in natural scenarios (e.g. see discussions of the influence of fO_2 on diffusion rates by Carlson (2006), Chu & Ague (2015) and Ferry *et al.* (2015)). Additionally, new concepts in metamorphic petrology offer an alternative explanation relating to maintenance of sharp compositional gradients as a result of significant, long-lived, grain-scale pressure variations and their influence on chemical activity and diffusion (e.g. Tajčmanová *et al.* 2014; Wheeler 2014).

Diffusion is central to geospeedometry, but is also a fundamental consideration for geochronology. In geochronology, diffusion is often treated by the 'closure temperature' concept of Dodson (1973), which calculates the *T*, for a mineral grain size and shape, cooled at a prescribed (uniform) rate, at which diffusive loss of the daughter isotope is fully compensated by radiogenic ingrowth; closure temperature gives the *T* during cooling to which a radiogenic age corresponds. The closure temperature model is an idealization that can misrepresent many real-world complexities, including multimodal grain size, non-linear or highly protracted cooling, and the effects of recrystallization during cooling (e.g. Lister & Baldwin 1996). Moreover, diffusion in geochronology (and geospeedometry) has been shown to be governed not only by *T*, but also by *P* (e.g. Harrison *et al.* 2009; Forster & Lister 2010, 2014; Warren *et al.* 2012*a*), deformation (e.g. Hames & Cheney 1997; Mulch *et al.* 2002; Kramer *et al.* 2003; Cosca *et al.* 2011) and the availability and nature of intergranular fluids (e.g. Rubie 1986, 1990; Kühn *et al.* 2000; Glodny *et al.* 2008; Smye *et al.* 2013).

To resolve the mismatch between metamorphic duration estimates produced from geochronology versus diffusion geospeedometry, future work must include more diffusion experiments that consider a broader set of conditions and the influence of additional variables (e.g. metamorphic *P*, presence of fluids, chemical activity, etc.). Ideally, future work would also utilize new, very high-precision approaches for the estimation of metamorphic time scales. These new approaches must allow assessment of the veracity of claims of extremely short-duration metamorphism that have been made on the basis of diffusion geospeedometry (e.g. Camacho *et al.* 2005; Ague & Baxter 2007; Viete *et al.* 2011*b*; Spear *et al.* 2012; Spear 2014).

Development of new very high-precision, petrologically controlled approaches to explore extremely short-duration metamorphism

The duration of thermal metamorphism is broadly governed by time scales for dissipation of the thermal anomaly that it records (see the introduction) and the thermal diffusivity of rock is far better characterized than rates of chemical diffusion. Thus, the method outlined in Figure 1 can provide a first-order check that the thermal length scale associated with a chemical diffusion feature matches the length scales of metamorphism observed in the field (e.g. Viete *et al.* 2011*a*). Such an approach may be used in cases where metamorphism is unambiguously driven by heating and the regional metamorphic sequence is relatively intact. However, it is of limited use where metamorphism occurs in isolated, dismembered blocks (e.g. high *P*/*T* blocks in a subduction mélange). For such cases, very high-precision, petrologically controlled geochronology techniques are necessary to verify the estimates of extremely short-duration metamorphism being made on the basis of diffusion geospeedometry.

The only study to have directly compared time scales of metamorphism obtained by diffusion geospeedometry with those estimated using high-precision geochronology has been that of Philippot *et al.* (2001). They showed that Lu–Hf garnet and $^{40}Ar/^{39}Ar$ white mica dates were within error, for metamorphism of both the *c*. 259 Ma Yukon–Tanana Terrane and *c*. 310 Ma Blyb Metamorphic Complex, Great Caucasus. For both cases, this limits the time scales for thermal metamorphism, during exhumation from intermediate–high *P*/*T* conditions, to less than the uncertainties on single Lu–Hf garnet and $^{40}Ar/^{39}Ar$ phengite dates; that is, a few million years. Diffusion geospeedometry performed on the same rocks yielded extremely short-duration metamorphic durations of a few hundred thousand years (Perchuk & Philippot 1997; Perchuk *et al.* 1999). Thus, Philippot *et al.* (2001) were able to demonstrate short-duration metamorphism for the Yukon–Tanana Terrane and Blyb Metamorphic Complex using high-precision geochronology, but not confirm the extremely short durations estimated from diffusion geospeedometry (Perchuk & Philippot 1997; Perchuk *et al.* 1999). They concluded that 'time-scale resolution required for unravelling rates of high-pressure metamorphism [estimated from diffusion geospeedometry] remains out of reach of current [geo] chronological methods' (Philippot *et al.* 2001, p. 24).

Cooper & Kent (2014) compared time scales of volcanic processes obtained from both diffusion geospeedometry and U-series geochronology, for 16 volcanic provinces. Geochronology was found to provide duration estimates 1 – 2 orders of magnitude longer than diffusion geospeedometry. Issues relating to errors in the Arrhenius parameters used for diffusion geospeedometry are less important for magmatic systems that, owing to high *T*, do not require significant down-temperature extrapolation from the conditions of experimental determination (e.g. Costa *et al.* 2008). However, diffusion is a *T*-dependent process and thus diffusion geospeedometry provides information on the time-integrated thermal response, but not the exact *T*–*t* history, which may include significant *T* fluctuations (particularly for a volcanic chamber experiencing periodic eruption and/or recharge). Cooper & Kent (2014) reasoned that the discrepancy in time scales between high-precision geochronology and diffusion geospeedometry may relate to episodicity in thermal processes. New approaches in geochronology capable of verifying extremely short-duration metamorphic time scales obtained from diffusion geospeedometry must use techniques with very high temporal resolution on young rocks (to ensure access to time scales <1 myr), but must simultaneously offer the spatial resolution necessary to decipher episodicity in thermal (and metamorphic) processes.

Results obtained from geochronology can be influenced by elemental and/or isotopic disequilibrium relating to inheritance of 'isotopically old' or daughter-element-rich chemistry as a result of (relict) mineral breakdown (e.g. Thöni 2002; Romer & Xiao 2005; Pollington & Baxter 2011), persistence of sub-microscopic relict mineral domains (e.g. Beltrando *et al.* 2013) or stagnant fluid conditions (e.g. Cosca *et al.* 2000; Warren *et al.* 2012*b*; Smye *et al.* 2013) during metamorphism. Dates obtained from geochronology may also be affected by elemental and/or isotopic fractionation during rapid, diffusion-limited mineral growth (e.g. Skora *et al.* 2006; Watson & Müller 2009). The various influences of *P*, deformation, fluids and reaction histories on results obtained from

geochronology also illustrate a need for detailed petrological understanding and characterization to stand at the forefront in geochronology endeavours (e.g. Vance *et al.* 2003; Villa & Williams 2013). 'Petrochronology' is a term that has been coined to describe geochronology performed with detailed petrological context in terms of *P–T* and reaction history.

There are three existing techniques in petrochronology with the spatial and temporal resolution to resolve multiple metamorphic episodes at 100 – 1000 kyr. These are: (1) Sm–Nd or Lu–Hf thermal ionization mass spectrometry (TIMS) performed on single growth sectors of metamorphic garnet (e.g. Baxter *et al.* 2002; Ducea *et al.* 2003; Lancaster *et al.* 2008; Pollington & Baxter 2010; Dragovic *et al.* 2012, 2015), (2) the 'asymptotes and limits' approach to identifying the effects of brief heating and/or limited recrystallization on $^{40}Ar/^{39}Ar$ step-heating spectra (e.g. Forster & Lister 2004, 2005; Lister & Forster 2016), and (3) petrologically controlled U–Pb depth profiling approaches, including single-shot laser ablation split stream (SS-LASS) inductively coupled plasma mass spectrometry (ICP-MS) petrochronology, capable of deciphering distinct, fine-scale episodes of accessory mineral growth (e.g. Smye & Stockli 2014; Viete *et al.* 2015; Stearns *et al.* 2016). U–Pb TIMS approaches that use partial acid digestion or focused ion beam (FIB) milling to isolate extremely small volumes of zircon or monazite (for analysis) may also offer necessary spatial and temporal resolution, but are still in the embryonic stages of their development (R. Ickert, pers. comm.). Figure 4 provides a summary of the three established, high-resolution and very high-precision petrochronology techniques listed above, with images and plots for each demonstrating how the metamorphic minerals record growth episodes at the microscopic scale, and the results that can be obtained.

The high-resolution and very high-precision petrochronology techniques of Figure 4 have never been applied in combination (and in parallel with detailed diffusion geospeedometry) on a common set of young rocks. Such work would allow the various techniques to be benchmarked and calibrated. It thus represents a crucial next step for knowledge development on the origins and significance of short-duration metamorphism. Further development of high-resolution and very high-precision petrochronology techniques (including the above-mentioned work to compare results obtained from the three established techniques) will assist not only in assessing the veracity of diffusion geospeedometry results and the integrity and relevance of extremely short-duration metamorphic time scale estimates, but also in providing data from nature that can be used to verify diffusion experiments.

Drivers for short- and extremely short-duration metamorphism

If new, high-resolution techniques in very high-precision petrochronology yield results in agreement with the extremely short time scales for metamorphism being obtained from diffusion geospeedometry, then regional metamorphism may occur on time scales that belie thermal length scales. There are two potential explanations for such observations. First, metamorphism involving thermal drivers may, locally, record small-scale (extremely short-duration) thermal perturbations that overprint the regional (short-duration) metamorphic event (e.g. Baxter *et al.* 2002; Ague & Baxter 2007; Viete *et al.* 2011*b*). Second, extremely short-duration metamorphism may be driven not by heating but by alternative metamorphic drivers whose influence dissipates more quickly than heat can by conduction.

With respect to metamorphism driven by heating on multiple time and length scales, a model incorporating self affinity in thermal behaviour is outlined below. This model appeals to focused, episodic heating to account for both extremely short-duration and short-duration metamorphism within the one tectonothermal framework. A brief background on alternative metamorphic drivers is also provided below.

Self affinity in metamorphic time scales?

The Barrovian sillimanite isograd occurs in close association with mafic igneous intrusions in NE Scotland (e.g. Fettes 1970; Pankhurst 1970; Ashworth 1975). Chinner (1966), Harte & Johnson (1969) and Harte & Hudson (1979) showed that the highest-*T* isograds (e.g. sillimanite, migmatite) appear to have been 'superimposed' on the regional Barrovian isograd pattern. Diffusion geospeedometry applied to the high-grade Barrovian rocks has yielded extremely short estimates for the duration of thermal metamorphism (Ague & Baxter 2007; Viete *et al.* 2011*b*).

Chinner (1966) considered the Barrovian sillimanite overprint to have a fundamentally different thermal origin from the broader regional Barrovian metamorphism. Harte & Hudson (1979) proposed an alternative model in which the sillimanite overprint developed within the same thermal context as the rest of the Barrovian metamorphic sequence; the sillimanite overprint represents the Barrovian thermal climax. Viete *et al.* (2013) reconciled the Harte & Hudson (1979) view on the sillimanite overprint with the spatial association between sillimanite-grade rocks and the Grampian gabbros, suggesting that the entire Barrovian thermal anomaly, from the chlorite zone to the sillimanite zone, resulted from regional contact metamorphism driven by punctuated and focused magmatic heat advection.

The punctuated heat advection model of Viete *et al.* (2013) followed Viete *et al.* (2011*b*), who showed that Mn diffusion is recorded at multiple, discrete length scales within single garnets from the Barrovian sillimanite zone. Viete *et al.* (2011*b*) suggested that multimodal distribution of length scales of chemical diffusion in high-grade garnets mirrors the multimodal distribution of length scales of the Barrovian isograds, and records thermal activity on multiple time scales in the high-grade core of the Barrovian metamorphic series. Viete *et al.* (2011*b*, 2013) proposed that the sillimanite overprint was, in effect, a 'last gasp' pulse of an episodic advective heating regime that produced the entire Barrovian metamorphic series.

Figure 5 illustrates a series of *T–t* paths that may develop in response to the episodic heating regime proposed for the Barrovian metamorphism by Viete *et al.* (2011*b*, 2013). The conceptual curves of Figure 5 demonstrate decreasing self affinity with distance from the heat source. Rocks immediately adjacent to the zone of punctuated heating (i.e. the sillimanite zone) would record extremely short-duration (small-length-scale) thermal excursions and thus a punctuated *T–t* history (Fig. 5). On the other hand, the signature of each individual, extremely short-duration thermal excursions would dissipate with distance from the central heating zone, meaning that rocks at greater distance (e.g. the biotite zone) record only a single, regional thermal excursion (Fig. 5).

The prograde phase of the (short-duration) regional metamorphism develops in response to extremely short-duration heating episodes that are closely spaced in time. Regional cooling begins when extremely short-duration heating episodes are no longer of great enough frequency to maintain the regional thermal anomaly. As the regional thermal anomaly develops and both thermal and chemical diffusion length scales grow, evidence of single, extremely short length-scale thermal or chemical perturbations in the Barrovian high-grade core would be consumed. However, records of extremely short-duration thermal excursions that occur during regional cooling (Fig. 5) would survive.

Diffusion geospeedometry may be applied to extremely short length-scale diffusion features related to single and retrograde, extremely short-duration thermal pulses. Such diffusion features are

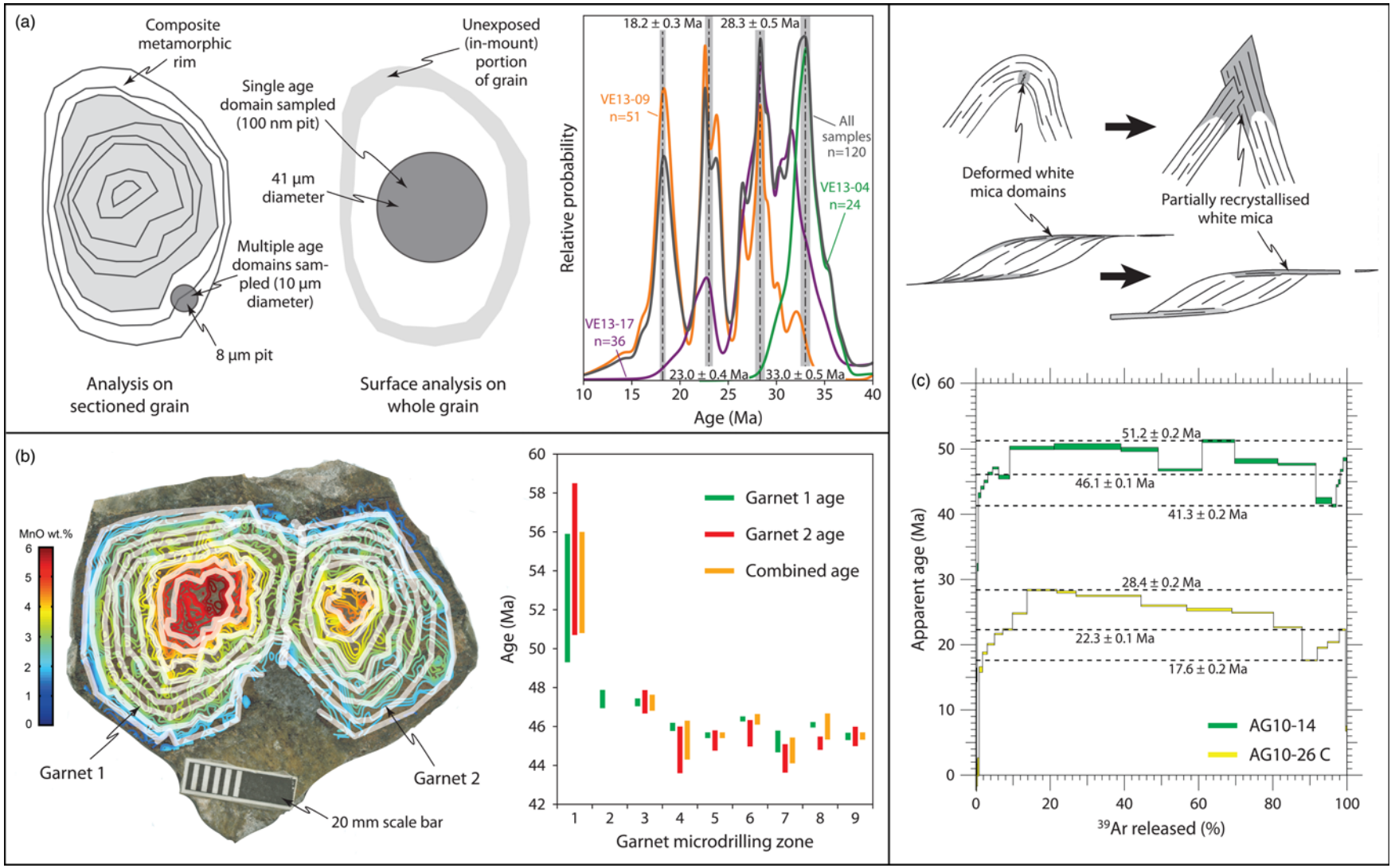

Fig. 4. Summary of three new very high-precision techniques for deciphering short-duration metamorphism: (**a**) U–Pb zircon SS-LASS ICP-MS approach of Viete *et al.* (2015); (**b**) microdrilling Sm–Nd TIMS approach of Pollington & Baxter (2010), Dragovic *et al.* (2012, 2015) and Gatewood *et al.* (2015); (**c**) asymptotes and limits $^{40}Ar/^{39}Ar$ white mica step-heating approach of Forster & Lister (2004). Results summarized in (**a**)–(**c**) are from Viete *et al.* (2015), Dragovic *et al.* (2015) and Lister & Forster (2016), respectively, and have been reproduced from the original files, with permission from the authors. Image of microdrilled garnets in (**b**) is from Dragovic *et al.* (2015, fig. 3, p. 113). Schematic illustration of recrystallized white mica in (**c**) is from Forster & Lister (2004, fig. 10, p. 300).

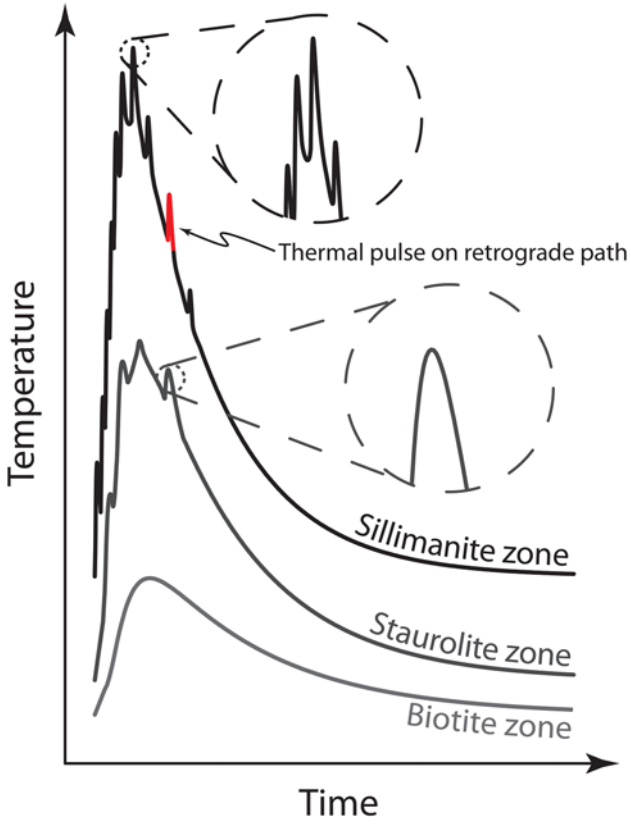

Fig. 5. Conceptual *T*–*t* curves for a thermal anomaly that develops in response to self-affine, punctuated heating. A noteworthy feature is decreasing self affinity in *T*–*t* curves with distance from the main heating zone, such that proximal (sillimanite-zone) rocks experience thermal pulses on multiple time scales but distal (biotite-zone) rocks witness only one, regional thermal pulse. Diffusion geospeedometry applied to the sillimanite-zone rocks may return misleading, extremely short metamorphic durations owing to consideration of late textures that develop during localized heating episodes on the retrograde path (see red *T* spike indicated) rather than those that record the entire regional event.

expected for the self-affine, punctuated heating regime illustrated in Figure 5. However, if the extremely short length-scale features are mistakenly thought to represent the regional metamorphism, then abnormally short metamorphic durations would be calculated from diffusion geospeedometry. Thus, a possible explanation for the contradictory (extremely short) durations being obtained for regional metamorphism is that diffusion geospeedometry has focused on records of small, very localized thermal perturbations rather than the regional thermal anomaly itself.

The above-described thermal regime requires a regional heat source that develops incrementally, as the result of extremely short-duration thermal pulses. Focused and episodic hot fluid pulses and/or mechanical heating represent alternative heat sources to episodic (sheeted) magmatism in the self-affine, punctuated heating model. Large-scale shear zones, whose episodic deformation history could result in punctuated heating relating to elevated permeability (hot fluid fluxing, magma emplacement) and/or strain rate (mechanical work), provide a logical environment for a self-affine thermal regime (Viete *et al.* 2011*b*, 2013). Non-uniform thermal tempo cannot, however, be explained by radiogenic heat production (which is a relatively constant-rate process), and can be explained by tectonic advection only if it involves very small-scale tectonic slices and is therefore associated with very thinly sliced lithostratigraphy. Thus, formal recognition of self-affine metamorphic tempo, involving metamorphic heating at multiple time and length scales, would help to rule out certain thermal drivers. An alternative explanation for extremely short-duration regional metamorphism is that metamorphism is triggered by drivers other than heating.

Alternative metamorphic drivers

Metamorphism need not record thermal activity. Numerous studies have observed episodic metamorphism as a result of near-isothermal burial or exhumation (e.g. García-Casco *et al.* 2002; Forster & Lister 2005; Beltrando *et al.* 2007; Kabir & Takasu 2010; Rubatto *et al.* 2011; Li *et al.* 2016; Lister & Forster 2016). Additionally, work on high *P*/*T* metamorphism has suggested that sudden metamorphism of otherwise metastable rocks can be triggered by episodic fluid fluxing (e.g. Kühn *et al.* 2000; Bjørnerud *et al.* 2002; John *et al.* 2004; Bjørnerud & Austrheim 2006; Glodny *et al.* 2008). Diffusion geospeedometry has typically been performed under the assumption that metamorphism is driven solely by heating, with the influence of *P* and fluid activity ignored. It may be that the extremely short-duration values being obtained from diffusion geospeedometry relate to a false assumption that metamorphism is principally driven by heating.

Episodicity, criticality and catastrophism

The science of geology is underpinned by the philosophy of uniformitarianism, which holds that the rock record should be interpreted in the context of current and observable processes, and which has entrenched observation as the primary tool for interpreting the Earth. Many natural phenomena involve processes observable at the Earth's surface and on human time scales. For example, it is accepted that earthquakes, volcanism and mass slides punctuate the longer-term processes of mountain building, secular cooling and topography creation. Although not directly observable, processes that occur at depth, such as regional metamorphism, may also involve inherently non-uniform and episodic activity.

Tables 1 and 2 and Figure 2 contain no record of Precambrian short-duration metamorphism. As discussed above, it is likely that limitations in geochronology have not allowed recognition of Archaean or Proterozoic short-duration metamorphism. Indeed, it could be argued that the evolution of geochronological precision has been integral in shaping ideas on the nature of metamorphism. When techniques in geochronology were first applied to metamorphism (in the 1960s–1980s), dates were calculated with precision >10 Ma. Metamorphism was thus thought to occur over time scales comparable with those generally accepted for orogenesis (i.e. 10 – 100 myr), and metamorphic facies series were considered to record relatively steady-state tectonothermal processes. Is it instead possible that orogenesis may persist only for the time scales of short-duration regional metamorphism (i.e. 1 – 10 myr)? Or that orogenesis is typified by bursts of short-duration tectonothermal activity that punctuate longer-term periods of relative tectonic quiescence (e.g. Lister *et al.* 2001)?

Techniques in geochronology are now resolving fine-scale metamorphic growth events on time scales of 1 – 10 myr, and the community appears to have accepted that regional metamorphism may not record long-lived tectonothermal environments. But extremely short-duration metamorphism involves episodicity at even shorter time scales (i.e. <1 myr). As tools in petrochronology and diffusion geospeedometry continue to develop, will we observe metamorphic episodicity at time scales of millennia, or less? For example, is it possible that rocks respond metamorphically to events as sudden and catastrophic as earthquakes? And, if so, why should metastability also occur, suggesting that rocks will respond to transient *P*–*T* pulses (on time scales $\ll$1 myr) yet fail to respond to ambient *P*–*T* conditions persisting over 10 – 100 myr?

In nature, reactions may require significant overstepping of equilibrium reaction boundaries, and therefore reaction rates may

significantly lag rates of change in P and/or T (e.g. Pattison & Tinkham 2009; Gaidies *et al.* 2011; Pattison *et al.* 2011; Spear *et al.* 2014). Rocks at the surface preserve assemblages formed at great P and T, suggesting that metamorphic transformation may be the exception rather than the rule. In a recent conversation with Paddy O'Brien, he quipped 'not only is metastability common, it is central to plate tectonics'. If metamorphism was slow and steady, rather than typified by metastability and episodicity, the density contrasts that drive plate tectonics may not occur. One may ponder whether plate tectonics (as we know it) would even exist if metamorphic facies series were to represent long-lived, quasi-steady-state tectonothermal environments.

Conclusions

Although the processes of plate tectonics undoubtedly lead to heat advection, the normal, ambient tectonothermal environment is not recorded in many regional metamorphic sequences. Instead, short-duration regional metamorphism records transient, atypical thermal episodes marking localized heat advection and/or production. The growing list of worldwide examples of short-duration regional metamorphism may necessitate a reassessment of the significance of metamorphic facies series.

Current techniques to quantify time scales of metamorphism yield conflicting results. Although metamorphic durations are commonly short, diffusion geospeedometry typically yields time scales $1-2$ orders of magnitude shorter than high-precision geochronology. In some cases, the extremely short-duration estimates obtained from diffusion geospeedometry belie the thermal length scales of regional metamorphism. This raises questions regarding sources and tempo for metamorphic heating and/or the nature of metamorphic drivers. Short- and extremely short-duration metamorphism also raises questions relating to episodicity and criticality in deep and thus unobservable processes.

Techniques in very high-precision petrochronology that are capable of resolving short- and even extremely short-duration metamorphic activity exist, but are yet to be applied in combination to a single set of young rocks. Such work represents a crucial next step for metamorphic geology, as it will allow comparison and appraisal of these new tools in very high-precision petrochronology, whilst simultaneously probing the veracity of diffusion geospeedometry's findings of extremely short-duration metamorphism.

Acknowledgements and Funding

Research funding from Durham University and Marie Curie actions of the European Commission, in the form of a Durham International Junior Research Fellowship to D.R.V., is gratefully acknowledged. Discussions with B. Hacker helped identify contradictions inherent in extremely short-duration metamorphism, and the need for development of new techniques in petrochronology. Feedback from L. White on an early draft helped improve the paper. The paper benefited greatly from thoughtful reviews by A. Smye and Subject Editor C. Clark. M. Allen both supported and encouraged the work. This paper was written in memory of Marco Beltrando.

Scientific editing by Chris Clark

References

Ague, J.J. & Baxter, E.F. 2007. Brief thermal pulses during mountain building recorded by Sr diffusion in apatite and multicomponent diffusion in garnet. *Earth and Planetary Science Letters*, **261**, 500–516.

Ashley, K.T., Thigpen, J.R. & Law, R.D. 2015. Prograde evolution of the Scottish Caledonides and tectonic implications. *Lithos*, **224–225**, 160–178.

Ashworth, J.R. 1975. The sillimanite zones of the Huntly–Portsoy area in the north-east Dalradian, Scotland. *Geological Magazine*, **112**, 133–136.

Ayres, M. & Vance, D. 1997. A comparative study of diffusion profiles in Himalayan and Dalradian garnets: constraints on diffusion data and the relative duration of the metamorphic events. *Contributions to Mineralogy and Petrology*, **128**, 66–80.

Bailey, E.H. 1962. Metamorphic facies of the Franciscan formation of California and their geologic significance. *In*: *Abstracts of papers submitted for six meetings with which the society was associated*. Geological Society of America, Special Papers, **68**, 4–5.

Bailey, E.H., Irwin, W.P. & Jones, D.L. 1964. *Franciscan and related rocks, and their significance in the geology of western California*. California Division of Mines Bulletin, **183**.

Baldwin, S.L., Monteleone, B.D., Webb, L.E., Fitzgerald, P.G., Grove, M. & Hill, E.J. 2004. Pliocene eclogite exhumation at plate tectonic rates in eastern Papua New Guinea. *Nature*, **431**, 263–267.

Barrow, G. 1893. On an intrusion of muscovite–biotite gneiss in the southeastern Highlands of Scotland and its accompanying metamorphism. *Quarterly Journal of the Geological Society of London*, **49**, 330–358, https://doi.org/10.1144/GSL.JGS.1893.049.01-04.52

Barrow, G. 1912. On the geology of Lower Dee-side and the southern Highland Border. *Geological Association of London Proceedings*, **23**, 274–290.

Barton, M.D. & Hanson, R.B. 1989. Magmatism and the development of low-pressure metamorphic belts: Implications from the western United States and thermal modelling. *Geological Society of America Bulletin*, **101**, 1051–1065.

Baxter, E.F. 2003. Natural constraints on metamorphic reaction rates. *In*: Vance, D., Müller, W. & Butler, I.M. (eds) *Linking the Isotopic Record with Petrology and Textures*. Geological Society, London, Special Publications, **220**, 183–202, https://doi.org/10.1144/GSL.SP.2003.220.01.11

Baxter, E.F., Ague, J.J. & DePaolo, D.J. 2002. Prograde temperature–time evolution in the Barrovian type-locality constrained by Sm/Nd garnet ages from Glen Clova, Scotland. *Journal of the Geological Society, London*, **159**, 71–82, https://doi.org/10.1144/0016-76901013

Beltrando, M., Hermann, J., Lister, G.S. & Compagnoni, R. 2007. On the evolution of orogens: pressure cycles and deformation mode switches. *Earth and Planetary Science Letters*, **256**, 372–388.

Beltrando, M., Di Vincenzo, G. & Ferraris, C. 2013. Preservation of sub-microscopic structural relicts in micas from the Gran Paradiso Massif (Western Alps): implications for ^{40}Ar–^{39}Ar geochronology. *Geochimica et Cosmochimica Acta*, **119**, 359–380.

Berman, R.G. 1988. Internally-consistent thermodynamic data for minerals in the system Na_2O–K_2O–CaO–MgO–FeO–Fe_2O_3–Al_2O_3–SiO_2–TiO_2–H_2O–CO_2. *Journal of Petrology*, **29**, 445–522.

Bickle, M.J., Hawkesworth, C.J., England, P.C. & Athey, D.R. 1975. A preliminary thermal model for regional metamorphism in the Eastern Alps. *Earth and Planetary Science Letters*, **26**, 13–28.

Bird, P., Toksöz, M.N. & Sleep, N.H. 1975. Thermal and mechanical models of continent–continent convergence zones. *Journal of Geophysical Research: Solid Earth*, **80**, 4405–4416.

Bjørnerud, M.G. & Austrheim, H. 2006. Hot fluids or rock in eclogite metamorphism? *Nature*, **440**, E4–E5.

Bjørnerud, M.G., Austrheim, H. & Lund, M.G. 2002. Processes leading to eclogitization (densification) of subducted and tectonically buried crust. *Journal of Geophysical Research: Solid Earth*, **107**, 2252, https://doi.org/10.1029/2001JB000527

Brouwer, F.M., van de Zedde, D.M.A., Wortel, M.J.R. & Vissers, R.L.M. 2004. Late-orogenic heating during exhumation: Alpine *PTt* trajectories and thermomechanical models. *Earth and Planetary Science Letters*, **220**, 185–199.

Burg, J.-P. & Gerya, T.V. 2005. The role of viscous heating in Barrovian metamorphism of collisional orogens: thermomechanical models and application to the Lepontine Dome in the Central Alps. *Journal of Metamorphic Geology*, **23**, 75–95.

Burton, K.W. & O'Nions, R.K. 1991. High-resolution garnet chronometry and the rates of metamorphic processes. *Earth and Planetary Science Letters*, **107**, 649–671.

Camacho, A., Lee, J.K.W., Hensen, B.J. & Braun, J. 2005. Short-lived orogenic cycles and the eclogitization of cold crust by spasmodic hot fluids. *Nature*, **435**, 1191–1196.

Carlson, W.D. 2006. Rates of Fe, Mg, Mn and Ca diffusion in garnet. *American Mineralogist*, **91**, 1–11.

Carslaw, H.S. & Jaeger, J.C. 1959. *Conduction of Heat in Solids*, 2nd edn. Clarendon Press, Oxford.

Catlos, E.J., Harrison, T.M., Kohn, M.J., Grove, M., Ryerson, F.J., Manning, C.E. & Upreti, B.N. 2001. Geochronologic and thermobarometric constraints on the evolution of the Main Central Thrust, central Nepal Himalaya. *Journal of Geophysical Research: Solid Earth*, **106**, 177–204.

Chakraborty, S. & Ganguly, J. 1992. Cation diffusion in aluminosilicate garnets: experimental determination in spessartine–almandine diffusion couples, evaluation of effective binary diffusion coefficients, and applications. *Contributions to Mineralogy and Petrology*, **111**, 74–86.

Chakraborty, S. & Rubie, D.C. 1996. Mg tracer diffusion in aluminosilicate garnets at 750–850°C, 1 atm. and 1300°C, 8.5 GPa. *Contributions to Mineralogy and Petrology*, **122**, 406–414.

Cherniak, D.J. & Ryerson, F.J. 1993. A study of strontium diffusion in apatite using Rutherford backscattering spectroscopy and ion implantation. *Geochimica et Cosmochimica Acta*, **57**, 4653–4662.

Cherniak, D.J., Watson, E.B. & Wark, D.A. 2007. Ti diffusion in quartz. *Chemical Geology*, **236**, 65–74.

Chinner, G.A. 1966. The distribution of pressure and temperature during Dalradian metamorphism. *Quarterly Journal of the Geological Society of London*, **122**, 159–186, https://doi.org/10.1144/gsjgs.122.1.0159

Christensen, J.N., Rosenfeld, J.L. & DePaolo, D.J. 1989. Rates of tectonometamorphic processes from rubidium and strontium isotopes in garnet. *Science*, **244**, 1465–1469.

Christensen, J.N., Selverstone, J., Rosenfeld, J.L. & DePaolo, D.J. 1994. Correlation by Rb–Sr geochronology of garnet growth histories from different structural levels within the Tauern Window, Eastern Alps. *Contributions to Mineralogy and Petrology*, **118**, 1–12.

Chu, X. & Ague, J.J. 2015. Analysis of experimental data on divalent cation diffusion kinetics in aluminosilicate garnets with application to timescales of peak Barrovian metamorphism, Scotland. *Contributions to Mineralogy and Petrology*, **170**, 25, https://doi.org/10.1007/s00410-015-1175-y

Chu, X., Ague, J.J., Axler, J.A. & Tian, M. 2016. Taconian retrograde eclogite from northwest Connecticut, USA, and its petrotectonic implications. *Lithos*, **240–243**, 276–294.

Clark, C., Fitzsimons, I.C.W., Healy, D. & Harley, S.L. 2011. How does the continental crust get really hot? *Elements*, **7**, 235–240.

Clark, C., Healy, D., Johnson, T., Collins, A.S., Taylor, R.J., Santosh, M. & Timms, N.E. 2015. Hot orogens and supercontinent amalgamation: a Gondwanan example from southern India. *Gondwana Research*, **28**, 1310–1328.

Collins, W.J. 2002. Hot orogens, tectonic switching, and creation of continental crust. *Geology*, **30**, 535–538.

Cooper, K.M. & Kent, A.J.R. 2014. Rapid remobilization of magmatic crystals kept in cold storage. *Nature*, **506**, 480–483.

Cosca, M.A., Giorgis, D., Rumble, D. & Liou, J.G. 2000. Limiting effects of UHP metamorphism on length scales of oxygen, hydrogen and argon isotope exchange: an example from the Qinglongshan UHP eclogites, Sulu Terrain, China. *International Geology Review*, **47**, 716–749.

Cosca, M., Stünitz, H., Bourgeix, A.L. & Lee, J.P. 2011. ^{40}Ar* loss in experimentally deformed muscovite and biotite with implications for ^{40}Ar/^{39}Ar geochronology of naturally deformed rocks. *Geochimica et Cosmochimica Acta*, **75**, 7759–7778.

Costa, F., Dohmen, R. & Chakraborty, S. 2008. Time scales of magmatic processes from modeling the zoning patterns of crystals. *In*: Putirka, K.D. & Tepley, F.J., III (eds) *Minerals, Inclusions and Volcanic Processes*. Mineralogical Society of America and Geochemical Society, Reviews in Mineralogy and Geochemistry, **69**, 545–594.

Dachs, E. & Proyer, A. 2002. Constraints on the duration of high-pressure metamorphism in the Tauern Window from diffusion modelling of discontinuous growth zones in eclogite garnet. *Journal of Metamorphic Geology*, **20**, 769–780.

De Yoreo, J.J., Lux, DR. & Guidotti, C.V. 1991. Thermal modelling in low-pressure/high-temperature metamorphic belts. *Tectonophysics*, **188**, 209–238.

Dodson, M.H. 1973. Closure temperature in cooling geochronological and petrological systems. *Contributions to Mineralogy and Petrology*, **40**, 259–274.

Dragovic, B., Samanta, L.M., Baxter, E.F. & Selverstone, J. 2012. Using garnet to constrain the duration and rate of water-releasing metamorphic reactions during subduction: an example from Sifnos, Greece. *Chemical Geology*, **314–317**, 9–22.

Dragovic, B., Baxter, E.F. & Caddick, M.J. 2015. Pulsed dehydration and garnet growth during subduction revealed by zoned garnet geochronology and thermodynamic modeling, Sifnos, Greece. *Earth & Planetary Science Letters*, **413**, 111–122.

Ducea, M.N., Ganguly, J., Rosenberg, E.J., Patchett, P.J., Cheng, W. & Isachsen, C. 2003. Sm–Nd dating of spatially controlled domains of single crystals: a new method of high-temperature thermochronology. *Earth and Planetary Science Letters*, **213**, 31–42.

Engi, M., Berger, A. & Roselle, G.T. 2001. Role of the tectonic accretion channel in collisional orogeny. *Geology*, **29**, 1143–1146.

England, P.C. 1978. Some thermal considerations of the Alpine metamorphism—past, present and future. *Tectonophysics*, **46**, 21–40.

England, P.C. & Richardson, S.W. 1977. The influence of erosion upon the mineral facies of rocks from different metamorphic environments. *Journal of the Geological Society, London*, **134**, 201–213, https://doi.org/10.1144/gsjgs.134.2.0201

England, P.C. & Thompson, A.B. 1984. Pressure–temperature–time-paths of regional metamorphism I. Heat transfer during the evolution of regions of thickened continental crust. *Journal of Petrology*, **25**, 894–928.

England, P.C., Le Fort, P., Molnar, P. & Pêcher, A. 1992. Heat sources for Tertiary metamorphism and anatexis in the Annapurna–Manaslu region, central Nepal. *Journal of Geophysical Research: Solid Earth*, **97**, 2107–2128.

Ernst, W.G. 1963. Petrogenesis of glaucophane schists. *Journal of Petrology*, **4**, 1–30.

Eskola, P. 1915. *On the relations between chemical and mineralogical composition in the metamorphic rocks of the Orijärvi region*. Bulletin de la Commission Géologique de Finlande, **44**.

Eskola, P. 1920. The mineral facies of rocks. *Norsk Geologisk Tidsskrift*, **6**, 143–194.

Eskola, P. 1939. Die metamorphen Gesteine. *In*: Barth, T.F.W., Correns, C.W. & Eskola, P. (eds) *Die Entstehung der Gesteine*. Springer, Berlin, 263–407.

Faryard, S.W. & Chakraborty, S. 2005. Duration of Eo-Alpine metamorphic events obtained from multicomponent diffusion modeling of garnet: a case study from the Eastern Alps. *Contributions to Mineralogy and Petrology*, **150**, 306–318.

Ferry, J.M., Stubbs, J.E., Xu, H., Guan, Y. & Eiler, J.M. 2015. Ankerite grains with dolomite cores: a diffusion chronometer for low- to medium-grade regionally metamorphosed clastic sediments. *American Mineralogist*, **100**, 2443–2457.

Fettes, D.J. 1970. The structural and metamorphic state of the Dalradian rocks and their bearing on the age of emplacement of the basic sheet. *Scottish Journal of Geology*, **6**, 108–117, https://doi.org/10.1144/sjg06010108

Forster, M.A. & Lister, G.S. 2004. The interpretation of ^{40}Ar/^{39}Ar apparent age spectra produced by mixing: application of the method of asymptotes and limits. *Journal of Structural Geology*, **26**, 287–305.

Forster, M.A. & Lister, G.S. 2005. Several distinct tectono-metamorphic slices in the Cycladic eclogite–blueschist belt, Greece. *Contributions to Mineralogy and Petrology*, **150**, 523–545.

Forster, M.A. & Lister, G.S. 2010. Argon enters the retentive zone: reassessment of diffusion parameters for K-feldspar in the South Cyclades Shear Zone, Ios, Greece. *In*: Spalla, M.I., Marotta, A.M. & Gosso, G. (eds) *Advances in Interpretation of Geological Processes: Refinement of Multi-scale Data and Integration in Numerical Modelling*. Geological Society, London, Special Publications, **332**, 17–34, https://doi.org/10.1144/SP332.2

Forster, M.A. & Lister, G.S. 2014. ^{40}Ar/^{39}Ar geochronology and the diffusion of ^{39}Ar in phengite–muscovite intergrowths during step-heating experiments *in vacuo*. *In*: Jourdan, F., Mark, D.F. & Verata, C. (eds) *Advances in ^{40}Ar/^{39}Ar Dating: from Archaeology to Planetary Sciences*. Geological Society, London, Special Publications, **378**, 117–135, https://doi.org/10.1144/SP378.16

Gaidies, F., Pattison, D.R.M. & de Capitani, C. 2011. Toward a quantitative model of metamorphic nucleation and growth. *Contributions to Mineralogy and Petrology*, **162**, 975–993.

Ganguly, J., Cheng, W. & Ganguly, J. 1998. Cation diffusion in aluminosilicate garnets: experimental determination in pyrope–almandine diffusion couples. *Contributions to Mineralogy and Petrology*, **131**, 171–180.

García-Casco, A., Torres-Roldán, R.L., Millán, G., Monié, P. & Schneider, J. 2002. Oscillatory zoning in eclogitic garnet and amphibole, Northern Serpentinite Melange, Cuba: a record of tectonic instability during subduction? *Journal of Metamorphic Geology*, **20**, 581–598.

Gasser, D., Rubatto, D., Bruand, E. & Stuwe, K. 2012. Large-scale short-lived metamorphism, deformation and magmatism in the Chugach metamorphic complex, southern Alaska: a SHRIMP U–Pb study of zircons. *Geological Society of America Bulletin*, **124**, 886–905.

Gatewood, M.P., Dragovic, B., Stowell, H.H., Baxter, E.F., Hirsch, D.M. & Bloom, R. 2015. Evaluating chemical equilibrium in metamorphic rocks using major element and Sm–Nd isotopic zoning in garnet, Townshend Dam, Vermont, USA. *Chemical Geology*, **401**, 151–168.

Giletti, B.J. 1974. Studies in diffusion I: Argon in phlogopite mica. *In*: Hofmann, A.W., Giletti, B.J., Yoder, H.S., Jr & Yund, R.A. (eds) *Geochemical Transport and Kinetics*. Carnegie Institution of Washington, Washington, DC, 107–115.

Glodny, J., Kühn, A. & Austrheim, H. 2008. Diffusion versus recrystallization processes in Rb–Sr geochronology: isotopic relics in eclogite facies rocks, Western Gneiss Region, Norway. *Geochimica et Cosmochimica Acta*, **72**, 506–525.

Graham, C.M. & England, P.C. 1976. Thermal regimes and regional metamorphism in the vicinity of overthrust faults: an example of shear heating and inverted metamorphic zonation from southern California. *Earth and Planetary Science Letters*, **31**, 142–152.

Hames, W.E. & Cheney, J.T. 1997. On the loss of ^{40}Ar* from muscovite during polymetamorphism. *Geochimica et Cosmochimica Acta*, **61**, 3863–3872.

Harley, S.L. 1998. On the occurrence and characterization of ultrahigh-temperature crustal metamorphism. *In*: Treloar, P.J. & O'Brien, P.J. (eds) *What Drives Metamorphism and Metamorphic Reactions?* Geological Society, London, Special Publications, **138**, 81–107, https://doi.org/10.1144/GSL.SP.1996.138.01.06

Harley, S.L. 2016. A matter of time: the importance of the duration of UHT metamorphism. *Journal of Mineralogical and Petrological Sciences*, **111**, 50–72.

Harrison, T.M. 1981. Diffusion of ^{40}Ar in hornblende. *Contributions to Mineralogy and Petrology*, **78**, 324–331.

Harrison, T.M., Ryerson, F.J., Le Fort, P., Yin, A., Lovera, O.M. & Catlos, E.J. 1997. A late Miocene–Pliocene origin for the central Himalayan inverted metamorphism. *Earth and Planetary Science Letters*, **146**, 1–7.

Harrison, T.M., Célérier, J., Aikman, A.B., Hermann, J. & Heizler, M.T. 2009. Diffusion of ^{40}Ar in muscovite. *Geochimica et Cosmochimica Acta*, **73**, 1039–1051.

Harte, B. & Hudson, N.F.C. 1979. Pelite facies series and the temperatures of Dalradian metamorphism in E Scotland. *In*: Harris, A.L., Holland, C.H. & Leake, B.E. (eds) *The Caledonides of the British Isles—Reviewed*. Geological Society, London, Special Publications, **8**, 323–337, https://doi.org/10.1144/GSL.SP.1979.008.01.36

Harte, B. & Johnson, M.R.W. 1969. Metamorphic history of Dalradian rocks in Glens Clova, Esk and Lethnot, Angus, Scotland. *Scottish Journal of Geology*, **5**, 54–80, https://doi.org/10.1144/sjg05010054

Hässig, M., Rolland, Y. *et al.* 2015. Multi-stage metamorphism in the South Armenian Block during the Late Jurassic to Early Cretaceous: tectonics over south-dipping subduction of northern branch of Neotethys. *Journal of Asian Earth Sciences*, **102**, 4–23.

Holland, T.J.B. & Powell, R. 1990. An enlarged and updated internally consistent thermodynamic dataset with uncertainties and correlations: the system K_2O–NaO–CaO–MgO–MnO–FeO–Fe_2O_3–Al_2O_3–TiO_2–SiO_2–C–H_2–O_2. *Journal of Metamorphic Geology*, **8**, 89–124.

Holland, T.J.B. & Powell, R. 1998. An internally-consistent thermodynamic dataset for phases of petrological interest. *Journal of Metamorphic Geology*, **16**, 309–343.

Holland, T.J.B. & Powell, R. 2011. An improved and extended internally consistent thermodynamic dataset for phases of petrological interest, involving a new equation of state for solids. *Journal of Metamorphic Geology*, **29**, 333–383.

Horton, F., Hacker, B., Kylander-Clark, A., Holder, R. & Jöns, N. 2016. Focused radiogenic heating of middle crust caused ultrahigh temperatures in southern Madagascar. *Tectonics*, **35**, https://doi.org/10.1002/2015TC004040.

Jamieson, R.A., Beaumont, C., Fullsack, P. & Lee, B. 1998. Barrovian regional metamorphism: where's the heat? *In*: Treloar, P.J. & O'Brien, P.J. (eds) *What Drives Metamorphism and Metamorphic Reactions?* Geological Society, London, Special Publications, **138**, 23–51, https://doi.org/10.1144/GSL.SP.1996.138.01.03

John, T., Scherer, E.E., Haase, K. & Schenk, V. 2004. Trace element fractionation during fluid-induced eclogitization in a subducting slab: trace element and Lu–Hf–Sm–Nd isotope systematics. *Earth and Planetary Science Letters*, **227**, 441–456.

Kabir, M.F. & Takasu, A. 2010. Evidence for multiple burial–partial exhumation cycles from the Onodani eclogites in the Sambagawa metamorphic belt, central Shikoku, Japan. *Journal of Metamorphic Geology*, **28**, 873–893.

Keay, S., Lister, G.S. & Buick, I.S. 2001. The timing of partial melting, Barrovian metamorphism and granite intrusion in the Naxos metamorphic core complex, Cyclades, Aegean Sea, Greece. *Tectonophysics*, **342**, 275–312.

Kelsey, D.E. 2008. On ultrahigh-temperature crustal metamorphism. *Gondwana Research*, **13**, 1–29.

Kelsey, D.E. & Hand, M. 2015. On ultrahigh temperature crustal metamorphism: phase equilibria, trace element thermometry, bulk composition, heat sources, timescales and tectonic settings. *Geoscience Frontiers*, **6**, 311–356.

Kemp, A.I.S., Shimura, T. & Hawkesworth, C.J. & EIMF, 2007. Linking granulites, silicic magmatism, and crustal growth in arcs: ion microprobe (zircon) U–Pb ages from the Hidaka metamorphic belt, Japan. *Geology*, **35**, 807–810.

Kohn, M.J. 2004. Oscillatory- and sector-zoned garnets record cyclic (?) rapid thrusting in central Nepal. *Geochemistry, Geophysics, Geosystems*, **5**, 12, https://doi.org/10.1029/2004GC000737

Kramer, N., Cosca, M., Buffat, P.A. & Baumgartner, L. 2003. Stacking fault-enhanced argon diffusion in naturally deformed muscovite. *In*: Vance, D., Müller, W. & Butler, I.M. (eds) *Linking the Isotopic Record with Petrology and Textures*. Geological Society, London, Special Publications, **220**, 249–260, https://doi.org/10.1144/GSL.SP.2003.220.01.15

Kretz, R. 1983. Symbols for rock-forming minerals. *American Mineralogist*, **68**, 277–279.

Kühn, A., Glodny, J., Iden, K. & Austrheim, H. 2000. Retention of Precambrian Rb/Sr phlogopite ages through Caledonian eclogite facies metamorphism, Bergen Arc Complex, W-Norway. *Lithos*, **51**, 305–330.

Lagos, M., Scherer, E.E., Tomaschek, F., Münker, C., Keiter, M., Berndt, J. & Ballhaus, C. 2007. High precision Lu–Hf geochronology of Eocene eclogite-facies rocks from Syros, Cyclades, Greece. *Chemical Geology*, **243**, 16–35.

Lancaster, P.J., Baxter, E.F., Ague, J.J., Breeding, C.M. & Owens, T.L. 2008. Synchronous peak Barrovian metamorphism driven by syn-orogenic magmatism and fluid flow in southern Connecticut, USA. *Journal of Metamorphic Geology*, **26**, 527–538.

Li, J.-L., Klemd, R., Gao, J. & John, T. 2016. Poly-cyclic metamorphic evolution of eclogite: evidence for multistage burial–exhumation cycling in a subduction channel. *Journal of Petrology*, **57**, 119–146.

Lister, G.S. & Baldwin, S.L. 1996. Modelling the effects of arbitrary *P–T–t* histories on argon diffusion in minerals using the MacArgon program for Apple Macintosh. *Tectonophysics*, **253**, 83–109.

Lister, G.S. & Forster, M.A. 2016. White mica $^{40}Ar/^{39}Ar$ age spectra and the timing of multiple episodes of high-pressure metamorphic mineral growth in the Cycladic eclogite–blueschist belt, Syros, Aegean Sea, Greece. *Journal of Metamorphic Geology*, **34**, 401–421.

Lister, G.S., Forster, M.A. & Rawlings, T.J. 2001. Episodicity during orogenesis. *In*: Miller, J.A., Holdsworth, R.R.E., Buick, I.S. & Hand, M. (eds) *Continental Reactivation and Reworking*. Geological Society, London, Special Publications, **184**, 89–113, https://doi.org/10.1144/GSL.SP.2001.184.01.06

Loomis, T.P., Ganguly, J. & Elphick, S.C. 1985. Experimental determination of cation diffusivities in aluminosilicate garnets. II. Multicomponent simulations and tracer diffusion coefficients. *Contributions to Mineralogy and Petrology*, **90**, 45–51.

McKenzie, D.P. 1967. Some remarks on heat flow and gravity anomalies. *Journal of Geophysical Research: Solid Earth*, **71**, 6261–6273.

McKenzie, D.P. 1969. Speculations on the consequences and causes of plate motions. *Geophysical Journal International*, **18**, 1–32.

Miyashiro, A. 1961. Evolution of metamorphic belts. *Journal of Petrology*, **2**, 277–311.

Miyashiro, A. 1973. *Metamorphism and Metamorphic Belts*. Allen & Unwin, London.

Miyashiro, A. 1994. *Metamorphic Petrology*. UCL Press, London.

Mottram, C.M., Warren, C.J., Regis, D., Roberts, N.M.W., Harris, N.B.W., Argles, T.W. & Parrish, R.R. 2014. Developing an inverted Barrovian sequence; insights from monazite petrochronology. *Earth and Planetary Science Letters*, **403**, 418–431.

Mottram, C.M., Warren, C.J., Halton, A.M., Kelley, S.P. & Harris, N.B.W. 2015. Argon behaviour in an inverted Barrovian sequence, Sikkim Himalaya: the consequences of temperature and timescale on $^{40}Ar/^{39}Ar$ mica geochronology. *Lithos*, **238**, 37–51.

Mulch, A., Cosca, M. & Handy, M. 2002. *In-situ* UV-laser $^{40}Ar/^{39}Ar$ geochronology of a micaceous mylonite: an example of defect-enhanced argon loss. *Contributions to Mineralogy and Petrology*, **142**, 738–752.

Müller, T., Cherniak, D.J. & Watson, E.B. 2012. Interdiffusion of divalent cations in carbonates: experimental measurements and implications for timescales of equilibration and retention of compositional signatures. *Geochimica et Cosmochimica Acta*, **84**, 90–103.

O'Brien, P.J. 1997. Garnet zoning and reaction textures in overprinted eclogites, Bohemian Massif, European Variscides: A record of their thermal history during exhumation. *Lithos*, **41**, 119–133.

O'Brien, S.C. & Vrana, S.S. 1995. Eclogites with a short-lived granulite facies overprint in the Moldanubian Zone, Czech Republic: petrology, geochemistry and diffusion modelling of garnet zoning. *Geologische Rundschau*, **84**, 473–488.

Oliver, G.J.H., Chen, F., Buchwaldt, R. & Hegner, E. 2000. Fast tectonometamorphism and exhumation in the type area of the Barrovian and Buchan zones. *Geology*, **28**, 459–462.

Oxburgh, E.R. & Turcotte, D.R. 1974. Thermal gradients and regional metamorphism in overthrust terrains with special reference to the Eastern Alps. *Schweizerische Mineralogische und Petrographische Mitteilungen*, **54**, 641–662.

Palin, R.M. & White, R.W. 2016. Emergence of blueschists on Earth linked to secular changes in oceanic crust composition. *Nature Geoscience*, **9**, 60–64.

Pankhurst, R.J. 1970. The geochronology of the basic igneous complexes. *Scottish Journal of Geology*, **6**, 83–107, https://doi.org/10.1144/sjg06010083

Parrish, R.R., Gough, S.J., Searle, M.P. & Waters, D.J. 2006. Plate velocity exhumation of ultrahigh-pressure eclogites in the Pakistan Himalaya. *Geology*, **34**, 989–992.

Pasyanos, M.E., Masters, T.G., Laske, G. & Ma, Z. 2014. LITHO1.0: an updated crust and lithospheric model of the Earth. *Journal of Geophysical Research: Solid Earth*, **119**, 2153–2172.

Pattison, D.R.M. & Tinkham, D.K. 2009. Interplay between equilibrium and kinetics in prograde metamorphism of pelites: an example from the Nelson aureole, British Columbia. *Journal of Metamorphic Geology*, **27**, 249–279.

Pattison, D.R.M., de Capitani, C. & Gaidies, F. 2011. Petrological consequences of variations in metamorphic reaction affinity. *Journal of Metamorphic Geology*, **29**, 953–977.

Penniston-Dorland, S.C., Kohn, M.J. & Manning, C.E. 2015. The global range of subduction zone thermal structure from exhumed blueschists and eclogites: rocks are hotter than models. *Earth and Planetary Science Letters*, **428**, 243–254.

Perchuk, A.L. & Philippot, P. 1997. Rapid cooling and exhumation of eclogitic rocks from the Great Caucasus, Russia. *Journal of Metamorphic Geology*, **15**, 299–310.

Perchuk, A.L. & Philippot, P. 2000. Geospeedometry and time scales of high-pressure metamorphism. *International Geology Review*, **42**, 207–223.

Perchuk, A.L., Philippot, P., Erdmer, P. & Fialin, M. 1999. Rates of thermal equilibration at the onset of subduction deduced from diffusion modeling of eclogitic garnets, Yukon–Tanana terrane, Canada. *Geology*, **27**, 531–534.

Philippot, P., Blichert-Toft, J., Perchuk, A. & Gerasimov, V. 2001. Lu–Hf and Ar–Ar chronometry supports extreme rate of subduction zone metamorphism deduced from geospeedometry. *Tectonophysics*, **342**, 23–38.

Platt, J.P., Soto, J.-I., Whitehouse, M.J., Hurford, A.J. & Kelley, S.P. 1998. Thermal evolution, rate of exhumation, and tectonic significance of metamorphic rocks from the floor of the Alboran extensional basin, western Mediterranean. *Tectonics*, **17**, 671–689.

Pollington, A.D. & Baxter, E.F. 2010. High resolution Sm–Nd garnet geochronology reveals the uneven pace of tectonometamorphic processes. *Earth and Planetary Science Letters*, **153**, 1–28.

Pollington, A.D. & Baxter, E.F. 2011. High precision microsampling and preparation of zoned garnet porphyroblasts for Sm–Nd geochronology. *Chemical Geology*, **281**, 270–282.

Pownall, J.M., Hall, R., Armstrong, R.A. & Forster, M.A. 2014. Earth's youngest known ultrahigh-temperature granulites discovered on Seram, eastern Indonesia. *Geology*, **42**, 279–282.

Raimbourg, H., Goffé, B. & Jolivet, L. 2007. Garnet reequilibration and growth in the eclogite facies and geodynamical evolution near peak metamorphic conditions. *Contributions to Mineralogy and Petrology*, **153**, 1–28.

Read, H.H. 1923. *Geology of the Country Round Banff, Huntley and Turriff. Memoir of the Geological Survey, Scotland Sheets 86 and 89*. HMSO, Edinburgh.

Read, H.H. 1952. Metamorphism and migmatisation in the Ythan Valley, Aberdeenshire. *Transactions of the Edinburgh Geological Society*, **15**, 265–279, https://doi.org/10.1144/transed.15.1.265

Reverdatto, V.V. & Polyansky, O.P. 2004. Modelling of the thermal history of metamorphic zoning in the Connemara region (western Ireland). *Tectonophysics*, **379**, 77–91.

Richardson, S.W. & Powell, R. 1976. Thermal causes of the Dalradian metamorphism in the central Highlands of Scotland. *Scottish Journal of Geology*, **12**, 237–268, https://doi.org/10.1144/sjg12030237
Romer, R.L. & Xiao, Y. 2005. Initial Pb–Sr(–Nd) isotopic heterogeneity in a single allanite–epidote crystal: implications of reaction history for the dating of minerals with low parent-to-daughter ratios. *Contributions to Mineralogy and Petrology*, **148**, 662–674.
Rubatto, D. & Hermann, J. 2001. Exhumation as fast as subduction? *Geology*, **29**, 3–6.
Rubatto, D., Regis, D., Hermann, J., Boston, K., Engi, M., Beltrando, M. & McAlpine, S.R.B. 2011. Yo-yo subduction recorded by accessory minerals in the Italian Western Alps. *Nature Geoscience*, **4**, 338–342.
Rubatto, D., Chakraborty, S. & Dasgupta, S. 2013. Timescales of crustal melting in the Higher Himalayan Crystallines (Sikkim, Eastern Himalaya) inferred from trace element-constrained monazite and zircon chronology. *Contributions to Mineralogy and Petrology*, **165**, 349–372.
Rubie, D.C. 1986. The catalysis of mineral reactions by water and restrictions on the presence of aqueous fluid during metamorphism. *Mineralogical Magazine*, **50**, 399–415.
Rubie, D.C. 1990. Role of kinetics in the formation and preservation of eclogites. *In*: Carswell, D.A. (ed.) *Eclogite Facies Rocks*. Blackie, Glasgow, 111–140.
Rudnick, R.L., McDonough, W.F. & O'Connell, R.J. 1998. Thermal structure, thickness and composition of continental lithosphere. *Chemical Geology*, **145**, 395–411.
Sandiford, M. & Powell, R. 1991. Some remarks on high-temperature–low-pressure metamorphism in convergent orogens. *Journal of Metamorphic Geology*, **9**, 333–340.
Schmitz, M.D. & Bowring, S.A. 2003. Ultrahigh-temperature metamorphism in the lower crust during Neoarchean Ventersdorp rifting and magmatism, Kaapvaal Craton, southern Africa. *Geological Society of America Bulletin*, **115**, 533–548.
Schwandt, C.S., Cygan, R.T. & Westrich, H.R. 1996. Ca self-diffusion in grossular garnet. *American Mineralogist*, **81**, 448–451.
Skora, S., Baumgartner, L.P., Mahlen, N.J., Johnson, C.M., Pilet, S. & Hellebrand, E. 2006. Diffusion-limited REE uptake by eclogite garnets and its consequences for Lu–Hf and Sm–Nd geochronology. *Contributions to Mineralogy and Petrology*, **152**, 703–720.
Smye, A.J. & Stockli, D.F. 2014. Rutile U–Pb depth profiling: a continuous record of lithospheric thermal evolution. *Earth and Planetary Science Letters*, **408**, 171–182.
Smye, A.J., Bickle, M.J., Holland, T.J.B., Parrish, R.R. & Condon, D.J. 2011. Rapid formation and exhumation of the youngest Alpine eclogites: a thermal conundrum to Barrovian metamorphism. *Earth and Planetary Science Letters*, **306**, 193–204.
Smye, A.J., Warren, C.J. & Bickle, M.J. 2013. The signature of devolatilisation: extraneous ^{40}Ar systematics in high-pressure metamorphic rocks. *Geochimica et Cosmochimica Acta*, **113**, 94–112.
Spear, F.S. 1993. *Metamorphic Phase Equilibria and Pressure–Temperature–Time Paths*. Mineralogical Society of America, Washington, DC.
Spear, F.S. 2014. The duration of near-peak metamorphism from diffusion modeling of garnet zoning. *Journal of Metamorphic Geology*, **32**, 903–914.
Spear, F.S., Ashley, K.T., Webb, L.E. & Thomas, J.B. 2012. Ti diffusion in quartz inclusions: implications for metamorphic time scales. *Contributions to Mineralogy and Petrology*, **164**, 977–986.
Spear, F.S., Thomas, J.B. & Hallett, B.W. 2014. Overstepping the garnet isograd: a comparison of QuiG barometry and thermodynamic modeling. *Contributions to Mineralogy and Petrology*, **168**, 1059–1073.
Stearns, M.A., Cottle, J.M., Hacker, B.R. & Kylander-Clark, A.R.C. 2016. Extracting thermal histories from the near-rim zoning in titanite using coupled U–Pb and trace-element depth profiles by single-shot laser-ablation split stream (SS-LASS) ICP-MS. *Chemical Geology*, **422**, 13–24.
Stern, R.J. 2005. Evidence from ophiolites, blueschists, and ultrahigh-pressure metamorphic terranes that the modern episode of subduction tectonics began in Neoproterozoic time. *Geology*, **33**, 557–560.
Stowell, H., Bulman, G., Tinkham, D. & Zuluaga, C. 2011. Garnet growth during crustal thickening in the Cascades crystalline core, Washington, USA. *Journal of Metamorphic Geology*, **29**, 627–647.
Stüwe, K. 1998. Heat sources of Cretaceous metamorphism in the Eastern Alps—a discussion. *Tectonophysics*, **287**, 251–269.
Tajčmanová, L., Podladchikov, Y., Powell, R., Moulas, E., Vrijmoed, J.C. & Connolly, J.A.D. 2014. Grain-scale pressure variations and chemical equilibrium in high-grade metamorphic rocks. *Journal of Metamorphic Geology*, **32**, 195–207.
Thompson, A.B. & England, P.C. 1984. Pressure–temperature–time-paths of regional metamorphism II. Their inference and interpretation using mineral assemblages in metamorphic rocks. *Journal of Petrology*, **25**, 929–955.
Thöni, M. 2002. Sm–Nd isotope systematics in garnet from different lithologies (Eastern Alps): age results, and an evaluation of potential problems for Sm–Nd chronometry. *Chemical Geology*, **185**, 255–281.
Toksöz, M.N. & Bird, P. 1977. Modelling of temperatures in continental convergence zones. *Tectonophysics*, **41**, 181–193.
Treloar, P.J. 1997. Thermal controls on early-Tertiary, short-lived, rapid regional metamorphism in the NW Himalaya, Pakistan. *Tectonophysics*, **273**, 77–104.
Treloar, P.J., O'Brien, P.J., Parrish, R.R. & Khan, M.A. 2003. Exhumation of early Tertiary, coesite-bearing eclogites from the Pakistan Himalaya. *Journal of the Geological Society, London*, **160**, 367–376, https://doi.org/10.1144/0016-764902-075
Turcotte, D.L. & Schubert, G. 2002. *Geodynamics*, 2nd edn. Cambridge University Press, Cambridge.
Turner, F.J. 1981. *Metamorphic Petrology: Mineralogical, Field and Tectonic Aspects*, 2nd edn. McGraw–Hill, New York.
Vance, D. & O'Nions, R.K. 1990. Isotopic chronometry of zoned garnets: growth kinetics and metamorphic histories. *Earth and Planetary Science Letters*, **97**, 227–240.
Vance, D. & O'Nions, R.K. 1992. Prograde and retrograde histories from the central Swiss Alps. *Earth and Planetary Science Letters*, **114**, 113–129.
Vance, E.F., Müller, W. & Villa, I.M. 2003. Geochronology: linking the isotopic record with petrology and textures—an introduction. *In*: Vance, D., Müller, W. & Butler, I.M. (eds) *Linking the Isotopic Record with Petrology and Textures*. Geological Society, London, Special Publications, **220**, 1–24, https://doi.org/10.1144/GSL.SP.2003.220.01.01
Vanderhaeghe, O., Teyssier, C. & Wysoczanski, R. 1999. Structural and geochronological constraints on the role of partial melting during the formation of the Shuswap metamorphic core complex at the latitude of the Thor–Odin dome, British Columbia. *Canadian Journal of Earth Sciences*, **36**, 917–943.
Viete, D.R., Richards, S.W., Lister, G.S., Oliver, G.J.H. & Banks, G.J. 2010. Lithospheric-scale extension during Grampian orogenesis in Scotland. *In*: Law, R.D., Butler, R.W.H., Holdsworth, R.E., Krabbendam, M. & Strachan, R.A. (eds) *Continental Tectonics and Mountain Building: The Legacy of Peach and Horne*. Geological Society, London, Special Publications, **335**, 121–160, https://doi.org/10.1144/SP335.7
Viete, D.R., Forster, M.A. & Lister, G.S. 2011*a*. The nature and origin of the Barrovian metamorphism, Scotland: ^{40}Ar/^{39}Ar apparent age patterns and the duration of metamorphism in the biotite zone. *Journal of the Geological Society, London*, **168**, 133–146, https://doi.org/10.1144/0016-76492009-164
Viete, D.R., Hermann, J., Lister, G.S. & Stenhouse, I.R. 2011*b*. The nature and origin of the Barrovian metamorphism, Scotland: diffusion length scales in garnet and inferred thermal time scales. *Journal of the Geological Society, London*, **168**, 115–132, https://doi.org/10.1144/0016-76492009-087
Viete, D.R., Oliver, G.J.H., Fraser, G.L., Forster, M.A. & Lister, G.S. 2013. Timing and heat sources for the Barrovian metamorphism, Scotland. *Lithos*, **177**, 148–163.
Viete, D.R., Kylander-Clark, A.R.C. & Hacker, B.R. 2015. Single-shot laser ablation split stream (SS-LASS) petrochronology deciphers multiple, short-duration metamorphic events. *Chemical Geology*, **415**, 70–86.
Villa, I.M. 2006. From nanometer to megameter: isotopes, atomic-scale processes, and continent-scale tectonic models. *Lithos*, **87**, 155–173.
Villa, I.M. 2016. Diffusion in mineral geochronometers: present and absent. *Chemical Geology*, **420**, 1–10.
Villa, I.M. & Williams, M.L. 2013. Geochronology of metasomatic events. *In*: Harlov, D.E. & Austrheim, H. (eds) *Metasomatism and the Chemical Transformation of Rock*. Springer, Berlin, 171–202.
Vorhies, S.H., Ague, J.J. & Schmitt, A.K. 2013. Zircon growth and recrystallization during progressive metamorphism, Barrovian zones, Scotland. *American Mineralogist*, **98**, 219–230.
Warren, C.J., Hanke, F. & Kelley, S.P. 2012*a*. When can muscovite ^{40}Ar/^{39}Ar dating constrain the timing of metamorphic exhumation? *Chemical Geology*, **291**, 79–86.
Warren, C.J., Smye, A.J., Kelley, S.P. & Sherlock, S.C. 2012*b*. Using white mica ^{40}Ar/^{39}Ar data as a tracer for fluid flow and permeability under high-*P* conditions: Tauern Window, Eastern Alps. *Journal of Metamorphic Geology*, **30**, 63–80.
Watson, E.B. & Müller, T. 2009. Non-equilibrium isotopic and elemental fractionation during diffusion-controlled crystal growth under static and dynamic conditions. *Chemical Geology*, **267**, 111–124.
Wheeler, J. 2014. Dramatic effects of stress on metamorphic reactions. *Geology*, **42**, 647–650.
Whitney, D.L., Teyssier, C., Fayon, A.K., Hamilton, M.A. & Heizler, M. 2003. Tectonic controls on metamorphism, partial melting and duration of regional metamorphism and magmatism in the Nigde Massif, Turkey. *Tectonophysics*, **376**, 37–60.
Whittington, A.G., Hofmeister, A.M. & Nabalek, P.I. 2009. Temperature-dependent thermal diffusivity of the Earth's crust and implications for magmatism. *Nature*, **458**, 319–321.
Wickham, S.M. & Oxburgh, E.R. 1985. Continental rifts as a setting for regional metamorphism. *Nature*, **318**, 330–333.
Wijbrans, J.R. & McDougall, I. 1986. ^{40}Ar/^{39}Ar dating of white micas from an Alpine high-pressure metamorphic belt on Naxos (Greece): the resetting of the argon isotopic system. *Contributions to Mineralogy and Petrology*, **93**, 187–194.
Wijbrans, J.R. & McDougall, I. 1988. Metamorphic evolution of the Attic Cycladic Metamorphic Belt on Naxos (Cyclades, Greece) utilizing ^{40}Ar/^{39}Ar age spectrum measurements. *Journal of Metamorphic Geology*, **6**, 571–594.
Yardley, B.W.D. 1989. *An Introduction to Metamorphic Petrology*. Longman, Harlow.